AD-A134 052 A COMPREHENSIVE DESCRIPTION OF THE MISSION SENSOR MICROWAVE IMAGER (SSM/I.. (U) NAVAL RESEARCH LAB WASHINGTON DC R C LO 30 SEP 83 NRL-MR-5199 1/1

UNCLASSIFIED F/G 12/1 NL

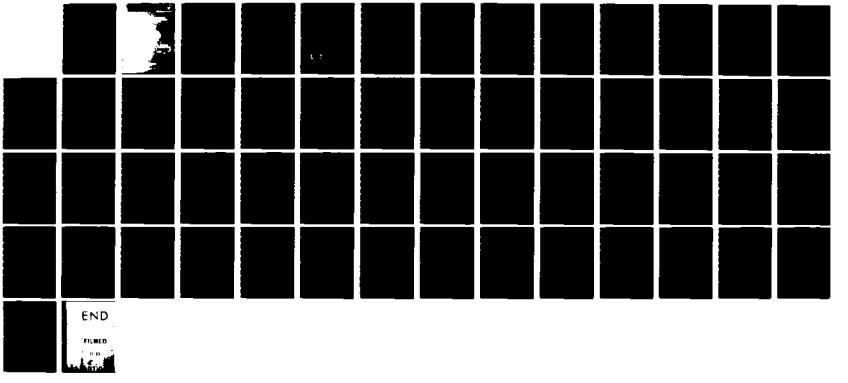

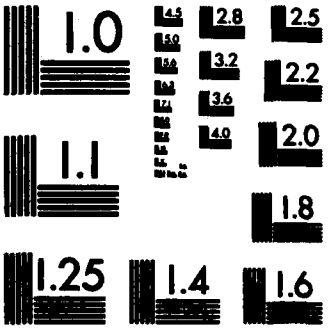

SECURITY CLASSIFICATION OF THIS PAGE *(When Data Entered)*

REPORT DOCUMENTATION PAGE		READ INSTRUCTIONS BEFORE COMPLETING FORM
1. REPORT NUMBER NRL Memorandum Report 5199	2. GOVT ACCESSION NO. A134052	3. RECIPIENT'S CATALOG NUMBER
4. TITLE *(and Subtitle)* A COMPREHENSIVE DESCRIPTION OF THE MISSION SENSOR MICROWAVE IMAGER (SSM/I) ENVIRONMENTAL PARAMETER EXTRACTION ALGORITHM		5. TYPE OF REPORT & PERIOD COVERED Interim report on a continuing NRL problem. 6. PERFORMING ORG. REPORT NUMBER
7. AUTHOR(s) R.C. Lo		8. CONTRACT OR GRANT NUMBER(s)
9. PERFORMING ORGANIZATION NAME AND ADDRESS Naval Research Laboratory Washington, DC 20375		10. PROGRAM ELEMENT, PROJECT, TASK AREA & WORK UNIT NUMBERS 35160N; SPW0524-CC; 79-1543-0-0
11. CONTROLLING OFFICE NAME AND ADDRESS Naval Space Systems Activity Los Angeles, CA 90009		12. REPORT DATE September 30, 1983 13. NUMBER OF PAGES 52
14. MONITORING AGENCY NAME & ADDRESS*(if different from Controlling Office)*		15. SECURITY CLASS. *(of this report)* UNCLASSIFIED 15a. DECLASSIFICATION/DOWNGRADING SCHEDULE

16. DISTRIBUTION STATEMENT *(of this Report)*

Approved for public release; distribution unlimited.

17. DISTRIBUTION STATEMENT *(of the abstract entered in Block 20, if different from Report)*

18. SUPPLEMENTARY NOTES

19. KEY WORDS *(Continue on reverse side if necessary and identify by block number)*

Parameters	SSM/I	Passive
Retrieval	Microwave	
Geophysical	Algorithm	

20. ABSTRACT *(Continue on reverse side if necessary and identify by block number)*

The Mission Sensor Microwave/Imager (SSM/I) is a passive microwave radiometric system designed to provide retrievals of the environmental parameters including sea surface wind, precipitation, atmospheric moisture content, soil moisture and sea ice conditions. It is a joint Navy/Air Force project developed by the Hughes Aircraft Company under the direction of the Navy Space Systems Activity (NSSA) and the Air Force Space Division to be flown on the Defense Meteorological Satellite Program (DMSP). The Space Sensing Applications Branch of → cont'd

(Continues)

DD FORM 1 JAN 73 1473 EDITION OF 1 NOV 65 IS OBSOLETE
S/N 0102-014-6601

SECURITY CLASSIFICATION OF THIS PAGE *(When Data Entered)*

20. ABSTRACT (Continued)

Cont → the Naval Research Laboratory has served as a technical consultant to NSSA beginning in fiscal year 1982.

Description of the environmental parameter retrieval technique, the geophysical model, the radiative transfer model and the parameter retrieval algorithms are presented. This information is designed to provide a comprehensive view of the SSM/I environmental parameter extraction algorithm for those individuals who have an interest in the geophysical data products from the SSM/I.

CONTENTS

ACKNOWLEDGMENTS iv

SECTION I. INTRODUCTION 1

SECTION II. THE DEVELOPMENT OF THE SSM/I EPE ALGORITHM 2

II.A. The D Matrix Approach 2
II.B. Separate Schemes for each Climate Zone 5
II.C. Piecewise Scheme 5

SECTION III. THE GEOPHYSICAL-RADIATIVE MODEL 8

III.A. The Radiative Transfer Model 8
III.B. The Atmosphere Model 13
III.C. The Surface Model 22

SECTION IV. RETRIEVAL OF GEOPHYSICAL PARAMETERS 30

IV.A. Piecewise Algorithm Criteria 30
IV.B. Ocean Retrievals 32
IV.C. Land Retrievals 40
IV.D. Ice Retrievals 44

REFERENCES 46

ACKNOWLEDGMENTS

The author wishes to thank Dr. Kenneth R. Hardy for providing information concerning the algorithms developed at the Environmental Research Technology, Inc. for the SSM/I. The guidance and discussions from Dr. James P. Hollinger are deeply appreciated. The author also appreciates the secretarial staff of the Space Sensing Applications Branch for typing the manuscript. This work would not have been possible without the support of CMDR T. M. Piwowar of the Navy Space Systems Activity.

A Comprehensive Description of the Mission Sensor Microwave Imager (SSM/I) Environmental Parameter Extraction Algorithm

I. INTRODUCTION

The Mission Sensor Microwave Imager (SSM/I) instrument and associated data processing software are being acquired as part of the joint Navy/Air Force project. It is a passive microwave radiometric system developed by the Hughes Aircraft Company (HAC) under the direction of the Navy Space Systems Activity (NSSA) and the Air Force Space Division to be flown on the Defense Meteorological Satellite Program (DMSP) operational spacecraft as an near all weather oceanographic and meteorological sensor.

The SSM/I is a seven-channel, four-frequency, linearly polarized, passive microwave radiometric system. The instrument measures atmospheric/surface brightness temperatures at 19.3, 22.2, 37.0 and 85.5 GHz (1). These data will be processed by the environmental parameter extraction (EPE) algorithm in place at the Fleet Numerical Oceanography Center (FNOC) and the Air Force Global Weather Center (AFGWC) to obtain near real time precipitation maps, sea ice morphology, marine surface wind speed, columnar integrated liquid water, and soil moisture percentage. These products will be distributed to Navy and Air Force DMSP operational sites to satisfy their unique mission requirements. They will also be made available to the general scientific and industrial communities through the shared METSAT data archival agreement between the National Oceanic and Atmospheric Administration (NOAA) and the Department of Defense (DOD).

The SSM/I data processing algorithm was developed at Environmental Research & Technology, Inc. (ERT) under a sub-contract from HAC. The algorithm is composed of four modules (2). The first module, SMISDP, ingests and processes raw satellite data to produce earth-located brightness temperatures (T_B's). The T_B's are then processed through the second module,

Manuscript approved August 10, 1983.

SMIEPE, which is the environmental parameter extraction algorithm, to produce estimates of ocean, land, ice, and atmospheric parameters. The third module, SMIVER, verifies the retrieved parameters against pre-selected climatology and ground truth fields. The last module, SMIUPD, updates the coefficients used in the parameter extraction algorithm when the verification results meet certain pre-determined criteria. Large volumes of documentation of the SSM/I data processing algorithm software and data files exist (e.g., 3,4,5).

The environmental parameter extraction module retrieves the environmental parameters using the brightness temperatures as independent variables in linear regression equations. The regression coefficients, which reside in a data file as part of the software system, are determined using geophysical models, radiative transfer models, an inversion algorithm, and climatology, which are not part of the SSM/I software. The documentation of these important components is scanty and often outdated (2,6,7,8).

The purpose of this report is to present a comprehensive digest of the EPE algorithm and the related models for those interested in the SSM/I and its applications. The substance for this report has been taken from all the previously mentioned references and a software listing of the geophysical models provided by Dr. Kenneth Hardy (9), the former leader of ERT's SSM/I team. This report includes an overview of the EPE algorithm, the geophysical models involved, and the coefficients and important criteria used in the development of the retrievals of environmental parameters.

II. THE DEVELOPMENT OF THE SSM/I EPE ALGORITHM

II.A The D Matrix Approach

The EPE algorithm, except for ice morphology, is based on the so-called D-matrix approach. It is a statistical method which chooses the most probable atmospheric and surface properties that produce the set of measured brightness temperatures (T_B's). The formalism for the statistical approach starts with the assumption that there exists some linear combination of T_B's which will provide information about the geophysical parameters in question.

That is to say:

$$P_i^* = \sum_{j=1}^{n} D'_{ij}\, T_j, \qquad \text{where } i = 1, \text{---}, m \quad .$$

or in vector form

$$\underline{P}^* = D'\, \underline{T}, \tag{II.1}$$

where P_i^* is the estimate of the i-th parameter P_i, T_j is the T_B of the j-th radiometric channel and D'_{ij} is the (i,j)-th element of the D matrix.

The $\underline{\underline{D}}$ matrix used in the SSM/I EPE algorithm is "tuned" to the average value of each parameter. This is accomplished by transforming the vector $\underline{T}$ into

$$\underline{\Phi}\,(\underline{T}) = (1,\ T_1 - \bar{T}_1,\ \text{----},\ T_n - \bar{T}_n). \tag{II.2}$$

The effect of this transformation is to add a column to the D matrix which contains the ensemble averages of the parameters.

$$\underline{P}^* = \underline{\underline{D}}\ \underline{\Phi}\,(\underline{T}), \tag{II.3}$$

where $\underline{\underline{D}}$ is the new D matrix with dimensions (m, n+1).

The elements of the D matrix are defined by minimizing the mean square error between the predicted and the actual values of the parameter P_i. It can be shown that

$$\underline{\underline{D}} = \underline{\underline{C}}\,(\underline{P}, \underline{\Phi}) \cdot \underline{\underline{C}}^{-1}\,(\underline{\Phi}, \underline{\Phi}), \tag{II.4}$$

where $\underline{\underline{C}}\,(\underline{P}, \underline{\Phi})$ is the correlation matrix between $\underline{P}$ and $\underline{\Phi}$ and $\underline{\underline{C}}^{-1}\,(\underline{\Phi}, \underline{\Phi})$ is the inverse of the auto-correlation matrix of $\underline{\Phi}$.

The development of the D matrix is demonstrated in Figure II.1. Radiosonde records and climatology are compiled to define the geophysical

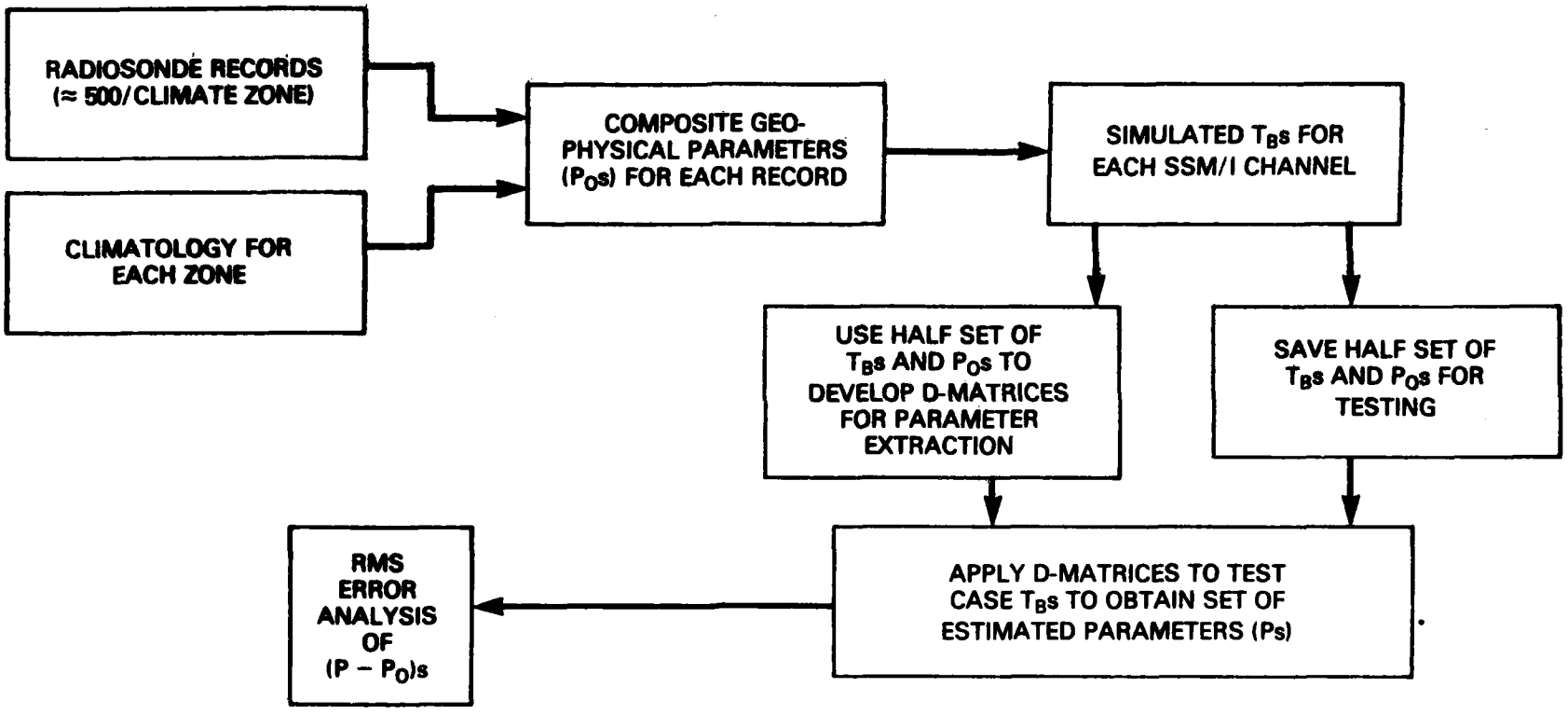

Figure II.1 SSM/I algorithm development

system including the atmosphere and the earth surface for radiative transfer calculations. A list of the desired environmental parameters is given in Table II.1. The atmosphere and surface data are used to simulate T_B's and thus $\underline{\phi}(\underline{T})$ through a geophysical-radiative model. Half of the $\underline{P}$ and $\underline{\phi}$ arrays are used to calculate correlation matrices and the D matrix (See equation II.4). The other half of the $\underline{\phi}$ array is used to test the validity of the D matrix by comparing the ground truth $\underline{P}$ to the estimated values, $\underline{P}^*$ which are calculated through equation II.3. The D matrices installed at FNOC and AFGWC have been tested with this procedure.

II.B Separate Schemes for Each Climate Zone

The assumption of linearity between $\underline{P}$ and $\underline{T}$ is not satisfied over the entire earth. Instead of adding higher order terms in the regression equations, a number of climate zones have been selected for the SSM/I EPE algorithm. For each of these zones, linearity is assumed. The climate zones are defined in Table II.2. A D matrix is developed for each of the climate zones. The D matrices of the transition zones, are averages of those of neighboring zones.

Due to the limitation of computing facilities at AFGWC, the maximum number of channels used for the retrieval of each parameter is limited to four. The channel selections for all the parameters are shown in Table II.1. For example, the regression equation for the sea surface wind speed is

$$SW = d_o + d_1\, T_B(19H) + d_2\, T_B(22V) + d_3\, T_B(37V) + d_4\, T_B(37H),$$

where $d_o, \ldots, d_4$ are D matrix coefficients. The value of the coefficients for each environmental parameter for all climate zones will be described in Section IV.

II.C Piecewise Scheme

Even though all the environmental parameters for each climate zone can be simultaneously extracted, the results may not be meaningful. For

Table II.1 Data Channel utilization table for SSM/I

PARAMETERS \ FREQUENCIES (GHz)			19		22	37		85	
			V	H	V	V	H	V	H
SW	SURFACE WIND SPEED, OCEAN			X	X	X	X		
RO	PRECIPITATION OVER OCEAN			X	X	X	X		
CWO	CLOUD WATER	OCEAN		X	X	X	X		
CWL		LAND	X	X		X		X	
LWO	LIQUID WATER	OCEAN		X	X	X	X		
LWL		LAND				X	X	X	X
SM	SOIL MOISTURE, LAND		X	X					
RL	PRECIPITATION OVER LAND					X	X	X	X
IC	SEA ICE CONDITIONS	CONCENTRATION				X	X		
IA		AGE				X			
IE		EDGE LOCATION							

TABLE II.2 Designation of SSM/I Climate Zones

		Jan	Feb	Mar	Apr	May	June	July	Aug	Sept	Oct	Nov	Dec
Trop	Land	3	3	3	3	1	1	1	1	1	1	3	3
	Ocean	4	4	4	4	2	2	2	2	2	2	2	2
Mid Lat	Land	9	9	5	5	5	7	7	7	5	5	5	9
	Ocean	10	10	6	6	6	8	8	8	6	6	6	10
Arctic	Land	13	13	13	13	11	11	11	11	11	11	13	13
	Ocean	14	14	14	14	12	12	12	12	12	12	14	14

1: tropical warm/land
2: tropical warm/ocean
3: tropical cool/land
4: tropical cool/ocean
5: mid lat spring-fall/land
6: mid lat spring-fall/ocean
7: mid lat summer/land
8: mid lat summer/ocean
9: mid lat winter/land
10: mid lat winter/ocean
11: arctic cool/land
12: arctic cool/ocean
13: arctic cold/land
14: arctic cold/ocean
15: transition zones

A. Lower Latitude transition zones (LLTS) are between tropics and mid lat.

a. LLTS warm/land
b. LLTS warm/ocean
c. LLTS cool/land
d. LLTS cool/ocean

B. Upper Latutide transition zones (ULTS) are between mid lat. and arctic

a. ULTS cool/land
b. ULTS cool/ocean
c. ULTS cold/land
d. ULTS cold/ocean

example, if there is heavy rain over land, the brightness temperatures will not be sensitive to the cloud water and soil moisture conditions. Similarly, when there is heavy rain over ocean, cloud water and sea surface wind retrievals would not be reliable. The SSM/I EPE algorithm employs the so-called piecewise scheme, to determine which parameters to retrieve based on the values of certain T_B observations. The piecewise schemes for ocean and land are depicted in Figures II.2 and II.3. The choice of parameters to retrieve is mainly based on rainfall. The criteria for determining whether there is no rain, light rain, or heavy rain are different for each climate zone. They are listed in Section IV.

The retrieval of ice parameters, including concentration and age, is accomplished through a deterministic approach. The ice algorithm is developed directly from physical relationships rather than through regression. The description of the physics of ice morphology and retrieval will be presented in Sections III and VI.

III. THE GEOPHYSICAL-RADIATIVE MODEL

The radiative transfer theory is used to simulate the brightness temperature obtained by a remote sensing platform, such as a satellite, observing the earth-atmosphere system. A geophysical model which specifies the physical and electromagnetic properties of the atmospheric and the earth's surface provides the necessary input parameters to the radiative transfer theory.

III.A The Radiative Transfer Model

For microwave radiation, the important atmospheric parameters are water vapor, oxygen and liquid water, both in the form of cloud water and rain. The form of the liquid water governs the method of calculation for the extinction coefficient and the solution to the radiative transfer equation. When liquid water exists in small droplets such as found in clouds, the attenuation is predominantly by absorption and calculations are relatively straightforward. But in the case of rain, water drops are so large that

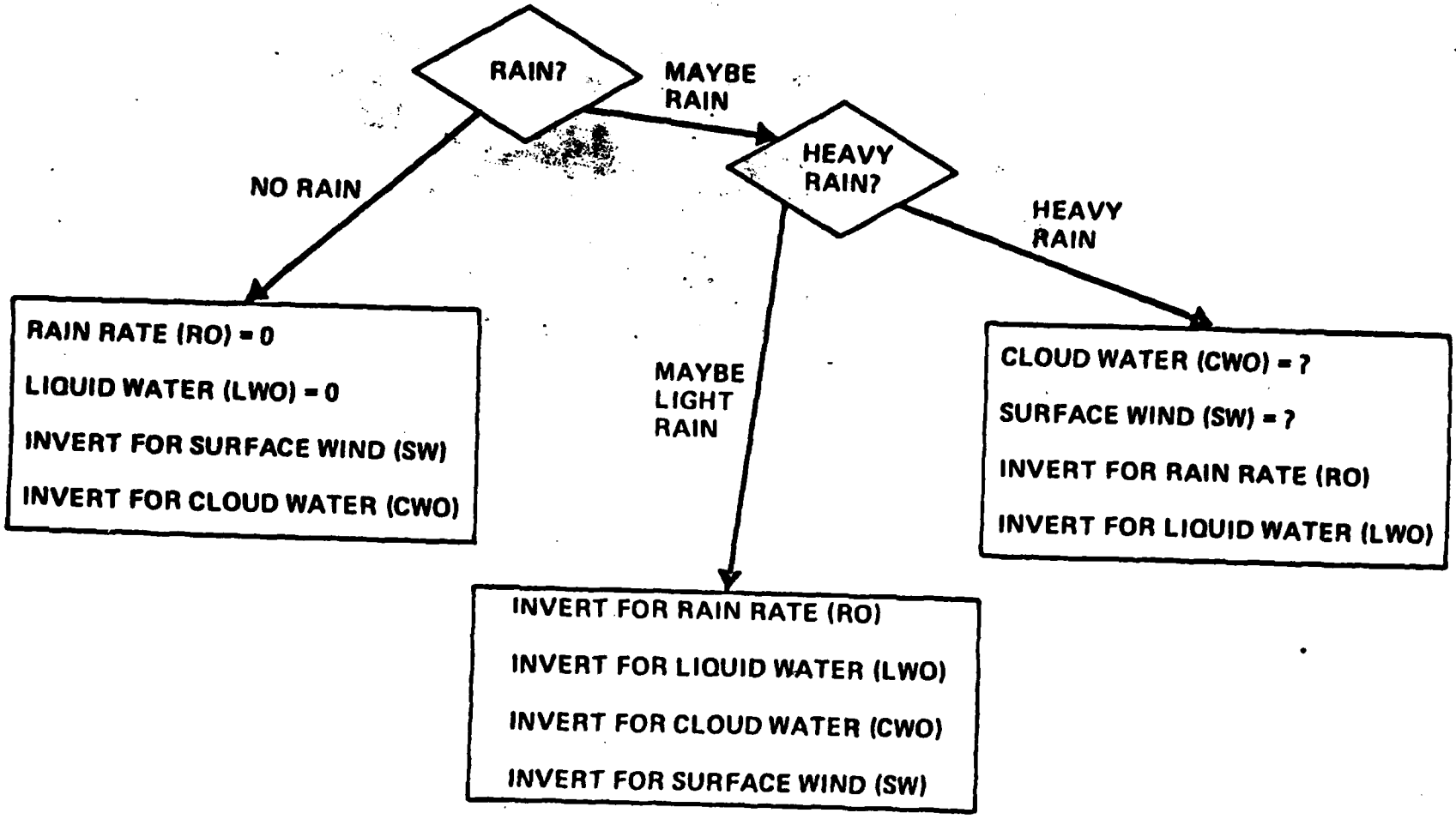

Figure II.2 Summary of piecewise algorithm over ocean

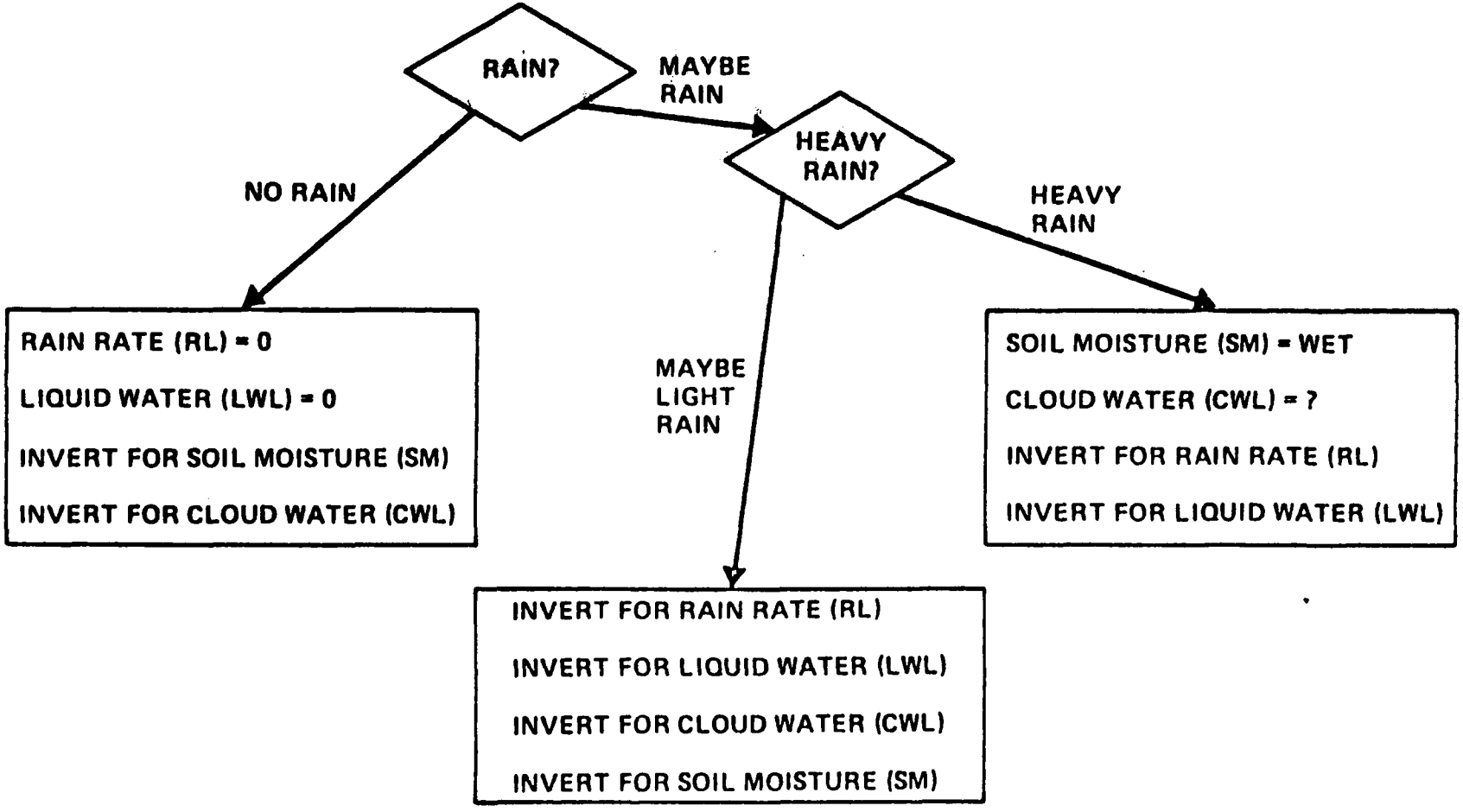

Figure II.3 Summary of piecewise algorithm over land

scattering effects must be considered. The Mie theory is employed to calculate the extinction coefficient including both absorption and scattering effects. An interative algorithm is needed to solve the radiative transfer equation.

The radiative transfer equation, with the Rayleigh-Jeans long wavelength approximation, for the intensity of thermal radiation from a blackbody can be written as

$$\frac{dT_B(Z,\theta)}{d\tau} = T_B(Z,\theta) - T(Z), \qquad \text{(III.1)}$$

where T_B is the brightness temperature, a function of height, Z, and of look angle θ. T is physical temperature and τ is the opacity. In the absence of scattering, the T_B sensed by a satellite can be expressed as (9)

$$T_B(Z,\theta) = T_{B_1}(Z,\theta) + [(1-R)T_G + R\,T_{B_2}]\, e^{-\tau}, \qquad \text{(III.2)}$$

where Z is the height of the satellite, R is the effective surface reflectivity, τ is the total opacity of the atmosphere along the line of sight (nepers) and T_G is the surface temperature (K). The quantities T_{B_1} and T_{B_2} are proportional to the upward emission from the atmosphere and the downward emission from the atmosphere plus attenuated sky background radiation and are given by

$$T_{B_1} = \int_0^Z T(z)\,\gamma(z)\, e^{\left(-\int_z^Z \gamma(z')\,\sec\theta\,dz'\right)} \sec\theta\,dz, \qquad \text{(III.3)}$$

$$T_{B_2} = T_{sky}\, e^{-\tau} + \int_0^Z T(z)\,(z)\, e^{\left(-\int_0^z \gamma(z')\,\sec\theta\,dz'\right)} \sec\theta\,dz, \qquad \text{(III.4)}$$

where $\tau = \int_0^Z \gamma(z)\ \sec\theta\ dz$ and $\gamma(z)$ is the total opacity at height z, representing the sum of contributions from water vapor, oxygen, and cloud water droplets.

Equations III.2 through III.4 are valid for all non-precipitating atmospheres. When precipitation is present multiple scattering effects are coupled with absorption. The Mie theory is based on the diffraction of a plane monochromatic wave by a sphere with a homogeneous, complex index of refraction. By examining the dissipation in the sphere and the scattered wave produced, it provides the information necessary for the calculation of the extinction coefficient and single scattering albedo.

The Mie efficiency factors for scattering, absorption and extinction are defined as the ratio of the actual to the geometric cross-sections.

$$Q_J = \chi_J/\pi r^2 \qquad J = \begin{cases} S \text{ (scattering)} \\ A \text{ (absorption)} \\ E \text{ (extinction)}, \end{cases} \tag{III.5}$$

where χ is the actual cross-section and r is the raindrop radius. By definition $Q_E = Q_A + Q_S$. The single scattering albedo is

$$\omega_o = Q_S/Q_A \tag{III.6}$$

The extinction coefficient is determined by integrating the efficiency factor over the drop size distribution encountered in the rain.

$$\gamma_E = \int N(r)\ Q_E\ (\tilde{n}\ (\lambda,T),\ \lambda,r)\ r^2 dr, \tag{III.7}$$

where N(r) is the number of drops of radius r per unit volume, λ is the observational wavelength, $\tilde{n}$ is the index of retraction and T is the temperature. The radiative transfer equation for the scattering medium can be written as

$$\mu \frac{dT_B(\tau',\mu)}{d\tau'} = T_B\ (\tau',\mu) - T_S(\tau',\mu)\ , \tag{III.8}$$

where μ is the cosine of the incidence angle, $\tau' = \tau/\mu$ and T_S is the source function

$$T_S = [1 - \omega_o(\tau')]\, T(\tau',\mu) - \frac{\omega_o(\tau')}{2} \int_{-1}^{1} p(\mu,\mu')\, T_B(\tau',\mu')\, d\mu', \qquad \text{(III.9)}$$

where P is the phase function. The integral equation for T_S can be written as

$$T_S(\tau) = [1-\omega_o(\tau)]\,(T - T_{sky}\, e^{-\tau}) + \frac{\omega_o(\tau)}{2}\int_o^{\tau^*} T_S(\tau)\, E_1(|\tau^* - \tau|)d\tau$$

$$+ \frac{\omega_o(\tau)}{2} E_2(\tau^* - \tau)\left[(1-R)\, T_G + R\int_o^{\tau^*} T_S(\tau)\, e^{\left[\frac{-(\tau^* - \tau)}{\mu}\right]} \frac{d\tau}{\mu}\right], \qquad \text{(III.10)}$$

where * is the total optical depth of the atmosphere and E_n is

$$E_n(x) = \int_o^1 e^{(-x/\mu)}\, \mu^{n-2}\, d\mu. \qquad \text{(III.11)}$$

A variational-iterative approach (10,11) is used for the solution of the source function T_S defined in equation (III.10).

III.B The Atmosphere Model

The physical electromagnetic properties of water vapor, oxygen, and liquid water as defined in the ERT model are described in this sub-section.

III.B.1 Water Vapor

The extinction coefficient due to water vapor as described by Gaut (12) is used. Laboratory measurements and theoretically generated data were used to examine and modify the expression formulated by Van Vleck and Weisskopf (13). Only the absorption line centered at 22.235 GHz is used to calculate the extinction coefficients for all but the highest frequency, i.e., 85.5 GHz, of the SSM/I instrument. The extinction due to water vapor is composed of two distinct portions; the resonance and non-resonance components. The

former is the rapidly changing contribution from the nearest water vapor absorption line while the latter is due to the slowly varying absorption wings of more distant lines.

$$\gamma_w(z) = \gamma_{w,RES}(z) + \gamma_{w,NON}(z)$$

$$= \left\{ k_1 \rho_w(z) \nu^2 T(z)^{-2.5} e^{[-644/T(z)]} \left[\frac{\Delta\nu}{(\nu-\nu_o)^2 + \Delta\nu^2} + \frac{\Delta\nu}{(\nu+\nu_o)^2 + \Delta\nu^2} \right] \right.$$

$$\left. + 5.k_2 \rho_w(z) \nu^2 T(z)^{-1.5} \Delta\nu \right\} \times 100 , \qquad \text{(III.12)}$$

where $\gamma_w(z)$ is the absorption due to water vapor at height z (nepers/m), ν is frequency (GHz), ν_o is the reference frequency (22.235 GHz) and k_1, k_2 are constants.

$$k_1 = 3.5175 \times 10^{-3}; \quad k_2 = 5.0920 \times 10^{-9}.$$

The half-width of the absorption line, $\Delta\nu$, is defined as

$$\Delta\nu = 2.62 (P(z)/P_o) (T(z)/T_o)^{-0.625} [1 + 0.15 \rho_w(z) T(z)/P(z)], \qquad \text{(III.13)}$$

where P(z) is pressure at height z (mb), P_o is 1013.25(mb), and T_o is 318.0 (K).

For 85.5 GHz, eight water vapor rotational spectral lines are included in the calculation of the absorption coefficient. The reference frequencies of these lines and other significant parameters are listed below.

i	ν_o	Stn(i)	$C_1(i)$	$C_2(i)$	$t_{exp}(i)$	$t_1(i)$	$t_2(i)$	Sp(i)
1	22.235	.0549	2.7057	.01976	.626	446.39	447.17	3
2	183.310	.1015	2.8800	.01906	.649	136.15	142.30	1
3	323.159	.0870	2.2956	.01952	.420	1283.02	1293.80	3
4	323.758	.0891	2.7876	.02050	.619	315.70	326.50	1
5	377.418	.1224	2.8440	.02102	.630	212.12	224.71	3
6	389.709	.0680	2.1060	.02035	.330	1525.31	1538.31	1
7	435.874	.0820	1.5000	.01976	.290	1045.14	1059.68	1
8	437.673	.0987	1.7700	.02253	.360	742.18	756.18	3

The resonance portion of the absorption coefficient, $\gamma_w(z)$, is given by

$$\gamma_{w,Res}(z) = \sum_{i=1}^{8} 45.5\ \rho_w(z)\ Sp(i)\ Stn(i)\left[\frac{\nu^2}{T(z)^{1.5}}\right] [\nu^2 - \nu_o^2(i)]\left[\frac{4\nu\cdot\Delta\nu}{(\nu^2 - \nu_o^2)^2 + 4\nu^2\Delta\nu^2}\right] t_m(i) \quad , \tag{III.14}$$

where Sp(i) is the spin mode and Stn(i) is the line strength.

$$\Delta\nu = C_1(i)\left(\frac{P(z)}{P_o}\right)\left(\frac{T_o}{T(z)}\right)^{t_{exp}(i)} [1 + C_2(i)\ \rho_w(z)\ T(z)/P(z)] \ , \tag{III.15}$$

where t_{exp} is the exponent for the temperature term and

$$tm = \exp\left[-1.43897\ \frac{t_1(i)}{T(z)}\right] - \exp\left[-1.43879\ \frac{t_2(i)}{T(z)}\right]$$

$$\text{if} \quad -1.43879\ \frac{[t_1(i) - t_2(i)]}{T(z)} \geq 0.1, \tag{III.16a}$$

$$tm(i) = \nu_o(i)\ \frac{0.04796}{T(z)}\ \exp\left[-1.43879\left(\frac{t_1(i)}{T(z)}\right)\right]$$

$$\text{if} \quad -1.43879\ \frac{[t_1(i) - t_2(i)]}{T(z)} \leq 0.1. \tag{III.16b}$$

The non-resonance term is defined as

$$\gamma_{w,Non}(z) = 1.2375 \times 10^{-9}\ \rho_w(z)\left(\frac{P(z)}{P_o}\right)\left(\frac{T_o}{T}\right)^{1.5 + \frac{\sum_{i=1}^{8} t_{exp}(i)}{8}} \cdot\nu^2, \tag{III.17}$$

and the total absorption due to water vapor is then

$$\gamma_w(z) = \gamma_{w,Res}(z) + \gamma_{w,Non}(z). \tag{III.18}$$

III.B.2 Oxygen

The Van Vleck and Weisskopf (13) formulation for the absorption line shape is adopted for the calculation of absorption due to oxygen.

$$\gamma_o(z) = C_1 P(z) (760/1013.25) T(z)^{-3} \cdot \nu^2$$

$$i = \sum_{1,45,2} \left\{ f_i^+ [i(2i+3)/(i+1)] + f_i^- [(i+1)(2i-1)/i] + 2 f_o [(i^2+i+1)(2i+1)/(i(i+1))] \right\} \cdot e^{-2.06844\, i(i+1)/T(z)} , \quad \text{(III.19)}$$

where $f_i^+ = \Delta\nu \left\{ 1/[(O^+(i) - \nu)^2 + \Delta\nu^2] + 1./[(O^+(i) + \nu)^2 + \Delta\nu^2] \right\}$

and

$$f_i^- = \Delta\nu \quad 1/[(O^-(i) - \nu)^2 + \Delta\nu^2] + 1./[O^-(i) + \nu)^2 + \Delta\nu^2] , \quad \text{(III.20)}$$

$$\Delta\nu = \alpha \cdot P(z)(0.21 + 0.78\, \xi) \left(\frac{300}{T(z)}\right)^{0.85} , \quad \text{(III.21)}$$

where $\xi = 0.25$ if $P(z) \geq 365.51$ mb

$\xi = 0.75$ $P(z) < 25.5$ mb

$$\xi = 0.25 + 0.5\, \ell n\left(\frac{365.51}{P(z)}\right) \Big/ \ell n\left(\frac{365.51}{25.5}\right), \text{ if } 25.5 \leq P(z) < 365.51;$$

$f_o = \Delta\nu / (\nu^2 + \Delta\nu^2)$;

$C_1 = 0.61576 \times 10^{-3}$;

$= (1.95 \times 760/1013.25) \times 10^{-3}$,

and $O^+(i)$ and $O^-(i)$ are line shape parameters for the absorption lines. They are defined by Rosenkrantz (15) and are listed in Table III.1.

The resonance portion of the absorption coefficient, $\gamma_w(z)$, is given by

$$\gamma_{w,Res}(z) = \sum_{i=1}^{8} 45.5\ \rho_w(z)\ Sp(i)\ Stn(i)\left[\frac{\nu^2}{T(z)^{1.5}}\right] [\nu^2 - \nu_o^2(i)] \left[\frac{4\nu \cdot \Delta\nu}{(\nu^2 - \nu_o^2)^2 + 4\nu^2\Delta\nu^2}\right] t_m(i) \quad , \tag{III.14}$$

where Sp(i) is the spin mode and Stn(i) is the line strength.

$$\Delta\nu = C_1(i)\left(\frac{P(z)}{P_o}\right)\left(\frac{T_o}{T(z)}\right)^{t_{exp}(i)} [1 + C_2(i)\ \rho_w(z)\ T(z)/P(z)] \ , \tag{III.15}$$

where t_{exp} is the exponent for the temperature term and

$$tm = \exp\left[-1.43897\ \frac{t_1(i)}{T(z)}\right] - \exp\left[-1.43879\ \frac{t_2(i)}{T(z)}\right]$$

$$\text{if} \quad -1.43879\ \frac{[t_1(i) - t_2(i)]}{T(z)} \geq 0.1, \tag{III.16a}$$

$$tm(i) = \nu_o(i)\ \frac{0.04796}{T(z)}\ \exp\left[-1.43879\left(\frac{t_1(i)}{T(z)}\right)\right]$$

$$\text{if} \quad -1.43879\ \frac{[t_1(i) - t_2(i)]}{T(z)} \leq 0.1. \tag{III.16b}$$

The non-resonance term is defined as

$$\gamma_{w,Non}(z) = 1.2375 \times 10^{-9}\ \rho_w(z)\left(\frac{P(z)}{P_o}\right)\left(\frac{T_o}{T}\right)^{1.5 + \frac{\sum_{i=1}^{8} t_{exp}(i)}{8}} \cdot \nu^2, \tag{III.17}$$

and the total absorption due to water vapor is then

$$\gamma_w(z) = \gamma_{w,Res}(z) + \gamma_{w,Non}(z). \tag{III.18}$$

III.B.2 Oxygen

The Van Vleck and Weisskopf (13) formulation for the absorption line shape is adopted for the calculation of absorption due to oxygen.

$$\gamma_o(z) = C_1 \, P(z) \, (760/1013.25) \, T(z)^{-3} \cdot \nu^2$$

$$i = \sum_{1,45,2} \left\{ f_i^+ [i(2i+3)/(i+1)] + f_i^- [(i+1)(2i-1)/i] + 2 f_o [(i^2+i+1)(2i+1)/(i(i+1))] \right\} \cdot$$

$$e^{-2.06844 \, i(i+1)/T(z)} \, , \qquad \text{(III.19)}$$

where $f_i^+ = \Delta\nu \left\{ 1/[(O^+(i) - \nu)^2 + \Delta\nu^2] + 1./[(O^+(i) + \nu)^2 + \Delta\nu^2] \right\}$

and

$$f_i^- = \Delta\nu \quad 1/[(O^-(i) - \nu)^2 + \Delta\nu^2] + 1./[O^-(i) + \nu)^2 + \Delta\nu^2] \, , \qquad \text{(III.20)}$$

$$\Delta\nu = \alpha \cdot P(z)(0.21 + 0.78 \, f)\left(\frac{300}{T(z)}\right)^{0.85} \, , \qquad \text{(III.21)}$$

where $= 0.25$ if $P(z) \geq 365.51$ mb

$= 0.75 \quad P(z) < 25.5$ mb

$$= 0.25 + 0.5 \, \ell n\left(\frac{365.51}{P(z)}\right) \Big/ \ell n\left(\frac{365.51}{25.5}\right), \text{ if } 25.5 \leq P(z) < 365.51;$$

$f_o = \Delta\nu / (\nu^2 + \Delta\nu^2)$;

$C_1 = 0.61576 \times 10^{-3}$;

$= (1.95 \times 760/1013.25) \times 10^{-3}$,

and $O^+(i)$ and $O^-(i)$ are line shape parameters for the absorption lines. They are defined by Rosenkrantz (15) and are listed in Table III.1.

TABLE III.1 Line Shape Parameters for the Absorption Due to Oxygen

i	$0^{+}(i)$	$0^{-}(i)$
1	56.2648	118.7505
3	58.4466	62.4863
5	59.5910	60.4863
7	60.4348	59.1642
9	61.1506	58.3239
11	61.8002	57.6125
13	62.4112	56.9682
15	62.9980	56.3634
17	63.5685	55.7839
19	64.1272	55.2214
21	64.6779	54.6728
23	65.2240	54.1294
25	65.7626	53.5960
27	66.2978	53.0695
29	66.8313	52.5458
31	67.3627	52.0259
33	67.8923	51.5091
35	68.4205	50.9949
37	68.9478	50.4830
39	69.4741	49.9730
41	70.0000	49.4648
43	70.5249	48.9582
45	71.0497	48.4530

III.B.3 Liquid Water

a. Cloud droplets

The absorption coefficients of cloud droplets for all frequencies except 85.5 GHz are calculated based on the formulation by Staelin, et. al. (14). When there is no precipitation,

$$\gamma_c(z) = C_w(z) \cdot 10^{[0.0122 \cdot (291 - T(z)) - 4.0]/(30/\nu)^2}, \qquad \text{(III.22)}$$

where $C_w(z)$ is the cloud water density at height z.

For the 85.5 GHz, the Raleigh-Jeans approximation is used for the calculation of the absorption coefficient

$$\gamma_c(z) = 1.88685 \times 10^{-3} \, C_w(z) \cdot I_f/(30/\nu), \qquad \text{(III.23)}$$

where I_f is the imaginary part of $(-m^2+1)/(m^2+2)$ and m is the complex index of the refraction of water.

The absorption of ice cloud particles is calculated according to the following formula, assuming the temperature is below freezing, or $T(z)<273.16$ K.

$$\gamma_c(z) = [0.2302585 \cdot C_w(z) \cdot 10^{-(5.11 + 0.145\sqrt{273.16-T})}]/(30/\nu). \qquad \text{(III.24)}$$

b. Precipitation

Precipitation is the primary contributor to atmospheric attenuation at microwave wavelengths. The attenuation results from both absorption and scattering by the hydrometeors. The magnitude of these processes depends upon wavelength, drop size distribution, and precipitation layer thickness.

In the case of light rain, when it is permissible to neglect the effect of multiple scattering, the attenuation due to precipitation can be calculated according to equation III.12 and III.18. The liquid water con-

tent and the rain rate are assumed to be related by the Marshall-Palmer distribution function

$$L_w = 1.28 \times 10^{-10} \pi \cdot \left(\frac{450\ RR^{.21}}{-3.67}\right)^{-4} , \qquad \text{(III.25)}$$

where L_w is liquid water content (gm/m^3) and RR is rain rate (mm/hr.)

For heavier rain, the multiple scattering effect will be included through the algorithm described in sub-section III.A, equations III.5 thru III.11. One of the essential elements for the algorithm is the drop size distribution. The empirically observed spectra of Laws and Parson (16) is used to fit the Deirmendjian drop size distribution for the SSM/I rain algorithm. The Deirmendjian distribution is defined as

$$n(r) = Ar^C e^{(-Br^{C_2})} , \qquad \text{(III.26)}$$

where n(r) is the drop size distribution ($cm^{-3}\mu m^{-1}$), r is the radius of raindrop (μm), and A and B are scale parameters.

$$A = \left(\frac{M\ C_2}{\frac{4\pi}{3}\rho_w \cdot 10^6}\right)\left(\frac{B}{r}\right)^{[(C_1 + 4)/C_2]} , \qquad \text{(III.27)}$$

where M is the total liquid water content (gm/m^3),

$$M_w = \rho_w \int_0^\infty \frac{4\pi}{3} r^3 n(r) dr, \qquad \text{(III.28)}$$

$$B = \left(\frac{C_1}{C_2}\right) r_o^{-C_2} , \qquad \text{(III.29)}$$

and r_o is the mode radius (μm). The shape parameters are C_1 and C_2. The former of these affects the distribution of the smaller radii while the latter affects the larger radii.

The analytical results from fitting the Laws-Parson empirical spectrum are:

$$M = 0.636\ (RR^{.881}) \quad (gm/cm^3), \text{ where RR is rain rate (mm/hr)},$$

$$r_o = 225 + 9.16\ (RR^{.881}), \quad (r_o)_{max} = 375 \quad (\mu m),$$

$$C_1 = 4.0, \tag{III.30}$$

$$C_2 = 0.70 - 0.00458 \quad (RR^{.881}), \quad (C_2)_{min} = .625.$$

This formulation relates the rain rate to mode radius and liquid water density. It parameterizes the distribution as a function of rain rate only and thus simplifies the solution to the Deirmendjian distribution. On the other hand, it still retains the sensitivity of scattering to drop size, which would be lost if the Marshall-Palmer distribution is used. Figure III.1 shows the good agreement between the Deirmendjian model and the Laws and Parson distributions.

For weak storms with low rain rate (RR $\leq$ 8 mm/hr), the ceiling for the rain layer is assumed to be the 0 C isotherm. For more intensive convective storms, the ceiling is usually higher with a super-cooled water layer on top. The thickness of the layer, Z_{inc}, depends on the intensity of convection. In the ERT algorithm, the thickness of the supercooled layer, ΔZ, for rain rates in excess of 8 mm/hr, is given as

$$\Delta Z = (RR - 8.0)\ Z_{inc};\ \Delta Z < \Delta Z_{max}, \tag{III.31}$$

where Z_{inc} and ΔZ_{max} are determined from climatology (17). The values used are given below:

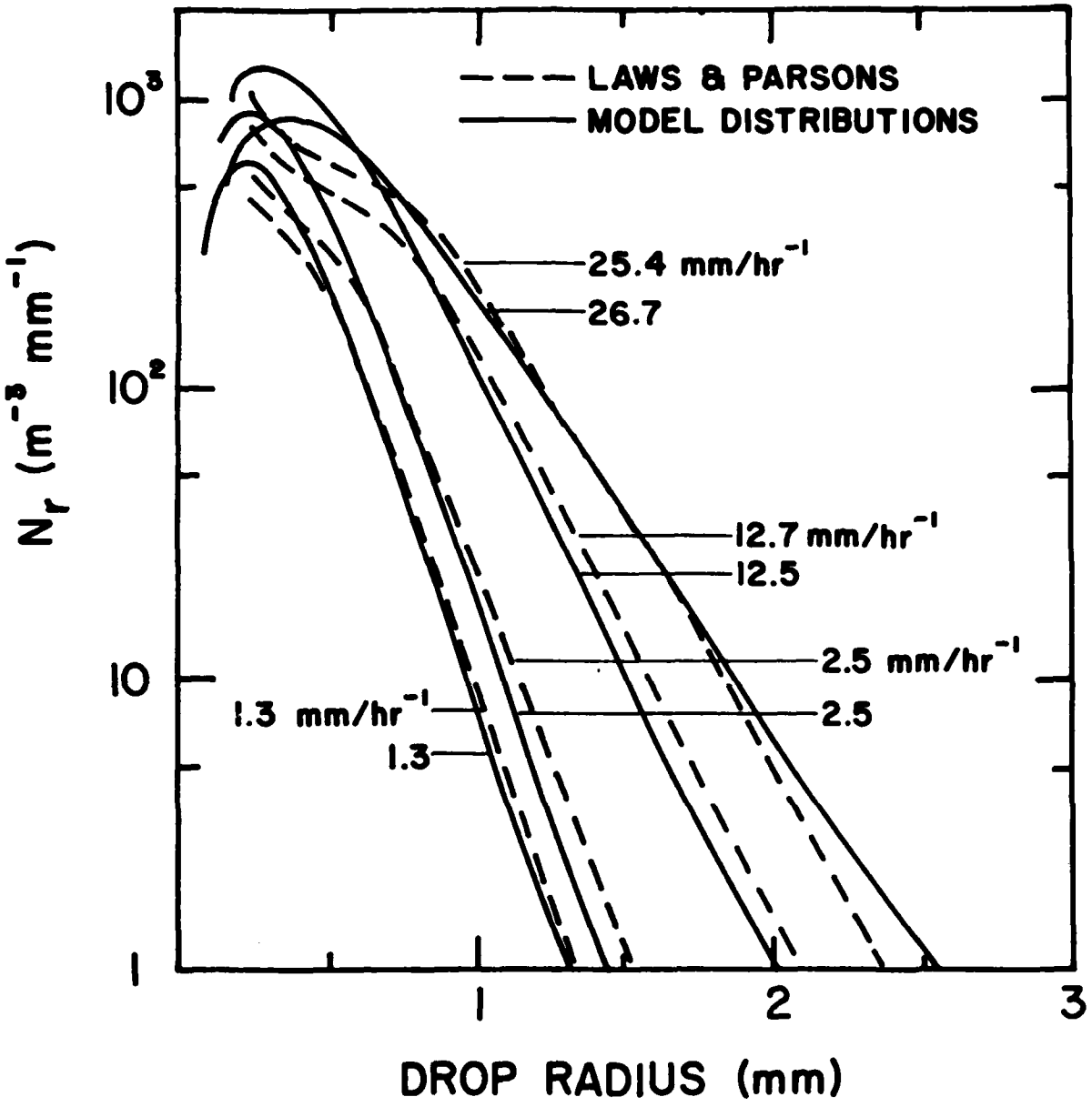

Figure III.1 The matching of the Deirmendjian raindrop size distribution used in model computations to the observed Laws and Parsons distributions.

		Z_{inc} $\frac{(m/hr)}{mm}$	ΔZ max (m)
Tropics	Land	50	800
	Ocean	50	800
Mid Lat	Land	100	1600
	Ocean	50	800
Arctic	Land	25	400
	Ocean	25	400

III.C The Surface Model

III.C.1 Ocean Surface

The calculation of the emissivity of a smooth water surface is relatively straightforward. The dielectric properties of sea water, derived from the measurements of Lane and Saxton (18) and expressed in analytical form by Chang and Wilheit (19) are used for the SSM/I algorithm. The Fresnel equations for a plane dielectric interface are used to calculate the emissivity of a smooth surface for a given view angle and polarization.

Wind driven waves and foam on the ocean surface both significantly alter the microwave emissivity of the ocean surface. Wind speed is highly variable both horizontally and vertically. Marine wind speed measured from a ship is usually referenced to a standard height of 20 meters. However, the wind speed which directly relates to roughness and foam is the friction velocity at the ocean–air interface. A relationship developed by Cardone (20) is used to extrapolate from the standard 20 meter height.

The ocean surface model developed by Wilheit (21) is adopted in the SSM/I algorithm. The roughness effect is modeled after Cox and Munk (22) treating the sea surface as a collection of plane facets large compared to the observational wavelength. The variance in sea surface slope is defined as a function of wind speed and then used for calculation of emissivity assuming a Gaussian slope distribution for the facets and using the Fresnel relations. The derived wind speed dependence of the surface slope variance, σ^2, is given by

$$\sigma^2(f) = (0.3 + 0.02f)\ (0.003 + 0.48w) \qquad \text{for } f < 35 \text{ GHz};$$
$$= 0.003 + 0.48w \qquad \text{for } f \geq 35 \text{ GHz}, \qquad \text{(III.32)}$$

where f is frequency in gigahertz (GHz) and w is the wind speed (m/sec) at 20 meter height.

Foam is treated as partially obscuring the surface in a manner independent of polarization but dependent upon frequency. The foam fraction, K, is defined as

$$K = 0.006\ (w - 7)\ (1 - e^{-f/7.5}) \qquad \text{for } w > 7 \text{ m/sec}$$
$$= 0 \qquad w \leq 7 \text{ m/sec}. \qquad \text{(III.33)}$$

This equation is based on Nordberg's (23) observation that the brightness temperature increases linearly with wind speed exceeding 7 m/sec, and that no foam forms below that wind speed.

III.C.2 Land Surface

The description of the land surface is extremely complex due to the many types of surfaces and the variation of the physical characteristics within each surface type. At present, the only land surface parameter retrieved by the SSM/I algorithm is the soil moisture for open land areas. Criteria have been developed to separate other land surface types such as forest and lakes from the open land areas.

The intensity of radiation from soil depends on the local dielectric constant and the physical temperature of the soil. Moisture produces a marked increase in both the real and the imaginary parts of the dielectric constant of soil, leading to a decrease in the soil emissivity. Experimental observations and theoretical calculations indicate that the emissivity of soil at microwave frequencies can range from >0.9 for dry soils to $\leq$0.6 for very moist soils.

A generalized incoherent layered surface model (24), was used to simulate expected SSM/I soil moisture brightness temperature signatures. Assume that there are N soil layers, with the atmospheric layer above and an

infinitely deep layer, with constant temperature and moisture content, below. The brightness temperature emerging at the soil surface for the horizontal polarization, T_{BH}, is given by

$$T_{BH} = \sum_{i=1}^{N} T(i)\, W(i)\, T_{RH}(i)\left[1 - e^{-g(i)\, dz(i)}\right]\left[1 + R_H(i) \cdot g(i)\, dz(i)\right], \quad \text{(III.34)}$$

where T(i) is the temperature of the i-th layer and dz(i) is the depth of the i-th layer. The weighting function w(i), is defined as

$$w(i) = e^{-\sum_{m=1}^{i=1} g(m)\, dz(m)}, \quad \text{(III.35)}$$

where $g(m) = 4\pi\nu/c \cdot A(m)$. Here c is the speed of light and $A(m) = \epsilon_I(m)/[2\, B(m)]$, where $\epsilon_I(m)$ is the imaginary part of the dielectric constant of the m-th layer.

$$B(m) = \left\{0.5\, Y(m) \cdot \left[1 + \left(1 + \left(\epsilon_I(m)/Y(m)\right)^2\right)^{1/2}\right]\right\}^{1/2}, \quad \text{(III.36)}$$

and $Y(m) = \epsilon_R(m) - \sin^2\theta$, where $\epsilon_R(m)$ is the real part of the dielectric constant of the m-th layer and θ is the incidence angle. The term, $T_{RH}(i)$, is the transmission factor of the i-th layer for horizontal polarization and is given by

$$T_{RH}(i) = [1 - R_H(1)].....[1 - R_H(i-1)], \quad \text{(III.37)}$$

where $R_H(i)$ is the horizontal extinction coefficient for the i-th layer.

$$R_H(i) = \left|\frac{C_{wv}(i) - C_{wv}(i+1)}{C_{wv}(i) + C_{wv}(i+1)}\right|^2, \text{ where } C_{wv}(i) = (B(i), A(i)). \quad \text{(III.38)}$$

The brightness temperature for vertical polarization, T_{BV}, emerging at the surface is

$$T_{BV} = \sum_{i=1}^{N} T(i)\, W(i)\, T_{RV}(i)\left[1 - e^{-g(i)\, dz(i)}\right]\left[1 + R_V(i)\, g(i)\, dz(i)\right]. \quad \text{(III.39)}$$

Here $T_{RV}(i)$ is the transmission factor of the i-th layer for vertical polarization;

$$T_{RV}(i) = (1 - R_V(1)\ (1 - R_V(2))\cdots\cdots(1 - R_V(i-1)), \qquad \text{(III.40)}$$

where $R_V(i)$ is the vertical extinction coefficient for the i-th layer.

$$R_V(i) = \left| \frac{\varepsilon(i)C_{wv}(i+1) - \varepsilon(i+1)\ C_{wv}(i)}{\varepsilon(i)C_{wv}(i+1) + \varepsilon(i+1)\ C_{wv}(i)} \right|^2 \text{, where } \varepsilon(i) = (\varepsilon_R(i), \varepsilon_I(i)). \qquad \text{(III.41)}$$

The dielectric constant is a function of frequency and soil moisture. For the 19.35 and 22.235 GHz channels, results from the study by Wang et.al. (25) are adopted. Let SM be soil moisture in percentage. The real part of the dielectric constant, ε_R, is given by

$$\begin{aligned} SM \le 7 \qquad & \varepsilon_R = 2.67 + 0.1\ SM, \\ 7 < SM \le 19.25 \qquad & \varepsilon_R = 3.37 + 0.78\ (SM - 7), \\ 19.25 < SM \qquad & \varepsilon_R = 12.92 + 0.23\ (SM - 19.25), \end{aligned} \qquad \text{(III.42)}$$

and for the imagniary part, ε_I, by

$$\begin{aligned} SM \le 10 \qquad & \varepsilon_I = 0.08\ SM, \\ 10 < SM \le 19 \qquad & \varepsilon_I = 0.80 + 0.57\ (SM - 10), \\ 19 < SM \qquad & \varepsilon_I = 5.93 + 0.28\ (SM - 19). \end{aligned} \qquad \text{(III.43)}$$

The results from the study by Geiger and Williams (26) are adopted for the dielectric constant of soil at 37.0 and 85.5 GHz. Here

$$\varepsilon_R = (1/0.885)(-2.8426 + 1.0534\ SM - 0.033808\ SM^2 + 3.434 \times 10^{-4}\ SM^3)$$

and (III.44)

$$\varepsilon_I = (1/0.885)(-1.2981 + 0.2925\ SM + 1.79 \times 10^{-3} SM^2 - 1.465 \times 10^{-4} SM^3).$$

At the higher frequencies, there is little sensitivity to soil moisture much below the earth surface. It suffices to calculate the reflection coefficient through the Fresnel coefficients using the dielectric constants specified above.

Choudhury and Schmugge (27) have developed a simple correction factor to the reflectivity to take the surface roughness into account. The corrected reflection coefficient is given by

$$R'(\theta) = R(\theta)\, e^{(-h \cos^2\theta)}, \qquad \text{(III.45)}$$

where

$$h = 4\sigma^2(2\pi/\lambda)^2.$$

σ^2 is the variance of the surface roughness, λ is the observational wavelength and h at 19.0 GHz is assumed to vary between 0 and 0.6.

III.C.3 Sea Ice

The upwelling brightness temperature of a scene containing sea water and various amounts of sea ice is a function of the ice concentration, ice emissivity, the physical temperatures of the ice components, and the amount of water vapor and liquid water in the atmosphere (6,7). The ice can be composed of first year (FY), multi-year (MY) or first-year thin ice (FT). The vertically polarized up-welling brightness temperature sensed by the SSM/I radiometer is expressed as

$$T_{BV} = e^{-\tau}\,[C\cdot F(\varepsilon_{fv}T_f + (1-\varepsilon_{fv})T_s) + C\cdot M(\varepsilon_{mv}T_m + (1-\varepsilon_{mv})T_s)$$
$$+ C(1-F-M)(\varepsilon_{tv}T_t + (1-\varepsilon_{tv})T_s) + (1-C)(\varepsilon_{wv}T_w + (1-\varepsilon_{wv})T_s)]$$
$$+ T_{atm}, \qquad \text{(III.46)}$$

where τ = total atmospheric opacity,

C = fraction of sea ice (includes all types within field of view),

F = fraction of FY ice relative to total ice present,

M = fraction of MY ice relative to total ice present,

$\epsilon_{fv}, \epsilon_{mv}, \epsilon_{tv}$ = vertically polarized surface emissivities of FY, MY and FT ice,

$_{wv}$ = vertically polarized surface emissivity of sea water,

T_f, T_m, T_t = surface temperature of FY, MY and FT ice,

T_w = surface temperature of sea water,

T_s = incident sky temperature at the surface due to atmospheric downward self-emission, and

T_{atm} = contribution from atmospheric upward self-smission.

An approximate expression for τ at a 50^o earth incidence angle for (ν = 6.6 to 37 GHz) is

$$\tau = \frac{2.384}{\lambda^2} L, \qquad \text{(III.47)}$$

where λ is the observational wavelength (cm) and L is the integrated vertical column of liquid water and water vapor (cm). An expression similar to equation III.46 exists for horizontal polarization. Ideally all SSM/I frequencies with different sea ice dependencies can be used to solve for C, F, and M simultaneously. However, limitations at the AFGWC computing facility prevent the use of all the SSM/I channels in a single algorithm. A simpler but reliable algorithm was developed.

Results from a study on ice emissivities (28) are presented in Table III.2. The difference between the vertical and horizontal emissivities at 37 GHz exhibits significantly less dependence on ice type than does the

Table III.2 Emissivity of ice

ICE TYPE	MY		FY ICE		FY THIN ICE		WATER CALM SEA	
POLARIZATION**	V	H	V	H	V	H	V	H
FREQ, GHZ								
19.35	0.86	0.73	0.97	0.84	0.96	0.78	0.60	0.33
37	0.69	0.64	0.97	0.95	0.96	0.87	0.70	0.40
37 (V-H)	0.05		0.02		0.09		0.30	

**V – VERTICAL; H – HORIZONTAL; 50° EARTH INCIDENCE ANGLE

polarization difference at 19.35 GHz. Furthermore, the polarization difference at 37 GHz is less sensitive to ice type than either the 37.0 GHz vertical or horizontal brightness temperatures. Therefore, the difference $T_{BV}(37) - T_{BH}(37)$ can be employed to obtain accurate estimates of ice concentration.

A sensitivity study was performed to determine the uncertainty of ice concentration using only the two 37 GHz channels (6,7). For winter conditions

$T_f = T_t = 260 \pm 10^{o}K$ $\quad\quad$ $\Delta\varepsilon = \varepsilon_v - \varepsilon_h = 0.05 \pm 0.05$

$T_m = 250 \pm 10^{o}K$ $\quad\quad$ $\lambda = 0.81$ cm

$T_w = 271K$

$L = 0.025 \pm 0.025$ cm,

and for instrument noise contributions of $\Delta T = 0$ K and $\Delta T = 1$ K, ice concentration retrieval accuracy ranges from 7% when C = 100% to 6% for low ice concentrations. The uncertainty for low ice concentration arises mainly from atmospheric variability, while for high ice concentration, variability in ice emissivity is the main source of uncertainty. These analyses indicate that the 37 GHz channels will provide an adequate margin for ice concentration measurements. Thus, the proposed algorithm to retrieve ice concentration, IC, is

$$IC = A_o + A_1 [T_{BV}(37) - T_{BH}(37)], \quad \text{(III.48)}$$

where A_o and A_1 are constants computed using equations III.46 and III.47 for the vertical polarization and equivalent equations for T_{BH}. Climatologically significant mean values of ice temperatures, atmospheric liquid water content, and mean values of ice emissivities are used as input to these equations. A_o and A_1 vary with season. They are presented in Section IV.

Dr. Rene Ramseier of the Atmospheric Environment Service of Canada has conducted many experiments to test the SSM/I ice algorithm using NIMBUS-7 SMMR 37.0 GHz data. Slight adjustments of coefficients were made to accommodate the difference in satellite geometry. Results from this study shows good agreement in ice concentration and ice edge between SSM/I ice

retrieval and ground truth data collected from reconnaissance flights, and surface observation.

Ice age determination (FY or MY) can be derived from the 37 GHz vertical brightness temperature value and computed value of ice concentration C. This is accomplished by computing the effective average ice brightness temperature and comparing it with known FY and MY T_B values. Let T_x be the effective average ice brightness temperature for vertical polarization.

$$T_x = \frac{e^{\tau}}{IC} [T_{BV} - T_{atm}] - \frac{1}{IC} (1-IC) [\epsilon_w T_w + (1 - \epsilon_w) T_s]. \quad \text{(III.49)}$$

With some algebraic manipulation, this reduces to

$$T_x = (C_o T_{BV} + C_1)/IC - C_2. \quad \text{(III.50)}$$

If T_x is greater than a predetermined value, ice age is designated as FY. The coefficients C_o, C_1 and C_2 are calculated based on climatological values. The criteria for determination of ice age together with these coefficients are presented in Section IV.

IV. RETRIEVAL OF GEOPHYSICAL PARAMETERS

Eleven climates are defined for the environmental parameter retrieval, for both the land and the ocean cases. These climates are defined in Table IV.1. A D matrix of regression coefficients is defined for each of the climates. Note that there are four transition climates within the eleven. The D matrices corresponding to these are derived from the neighboring climates. For the sake of convenience, code numbers are designated for each of these climates (see Table IV.1).

IV.A Piecewise Algorithm Criteria

The piecewise algorithm employed for the SSM/I environmental parameter retrieval is described in Subsection II.C. It checks certain criteria to

TABLE IV.1 Definition of Climate Codes

Climate Code No.	Definition
1	Tropical-warm
2	Tropical-cool
3	Lower Latitude Transition-warm
4	Lower Latitude Transition-cool
5	Mid. Lat.-Spring/Fall
6	Mid. Lat.-Summer
7	Mid. Lat.-Winter
8	Upper Lat. Transition-cool
9	Upper Lat. Transition-cold
10	Polar-cool
11	Polar-cold

determine which parameters to retrieve and which not to. It is designed to avoid meaningless retrievals and to use computing facilities most effectively. The criteria given for ocean cases include the critical temperature of the 19.35 H brightness temperature for the 'maybe rain' case CMRO, and the critical brightness temperature difference between the two polarizations of the 37 GHz frequency for 'maybe rain', CMRDO. When either of the two criteria is met, i.e., when T_B (19H) is greater than CMRO or when $T_B(37V) - T_B(37H)$ is less than CMRDO, the algorithm assumes that there is rain. The criterion for 'heavy rain' over the ocean, CHRDO, is also based on the difference in T_B between the two 37.0 GHz channels. When $T_B(37V) - T_B(37H)$ is less than CHRDO, the 'heavy rain' condition is assumed.

For land retrievals, there is a criterion, CFGL, defined to test for frozen ground. If $T_B(37V)$ is less than CFGL, the algorithm assumes frozen ground and considers soil moisture retrieval impossible. The retrieval algorithm also examines the 37 GHz brightness temperatures for 'heavy rain' using the criteria CHRL and CHRDL. The vertical channel brightness temperature is checked against the criterion CHRL. If it is less than CHRL and the difference between the two polarizations is less than CHRDL, 'heavy rain' is assumed and both the soil moisture and the cloud liquid water over land will not be retrieved. If the 'heavy rain' condition is not met, the algorithm then checks the 37 GHz brightness temperatures using criteria CMRL and CMRDL in a similar way to CHRL and CHRDL for the 'maybe rain' condition. If no rain is indicated, the rain rate over land and the liquid water over land are set to zero. The piecewise algorithm criteria are listed in Table IV.2 for the eleven climates.

IV.B Ocean Retrievals

IV.B.1 Ocean Surface Wind Speed (SW)

The response of brightness temperature at 19.35 H & V, 22.235 V, and 37 V & H to ocean surface wind speed is demonstrated in Figure IV.1 for a tropical clear atmosphere. The calculations are made at the look angle of the SSM/I. Note that the horizontal channels are more sensitive to wind

TABLE IV.2 Criteria for the Piecewise Algorithm

Climate Code	CMRO	CMRDO	CHRDO	CFGL	CHRL	CHRDL	CMRL	CMRDL
1	190	25	10	150	273	10	263	5
2	190	25	10	150	273	10	263	5
3	190	25	10	150	273	10	263	5
4	190	25	10	150	273	10	263	5
5	170	25	20	240	270	10	240	--
6	190	25	15	150	270	10	263	5
7	160	30	20	240	270	10	240	--
8	150	35	20	240	270	10	240	--
9	140	35	20	270	270	--	270	--
10	150	35	20	240	270	10	240	--
11	140	35	20	270	270	--	270	--

CMRO = Criterion for maybe rain over ocean for $T_B(19H)$

CMRDO = Criterion for maybe rain over ocean for $T_B(37V) - T_B(37H)$

CHRDO = Criterion for heavy rain over ocean for $T_B(37V) - T_B(37H)$

CFGL = Criterion for frozen ground for $T_B(37V)$

CHRL = Criterion for heavy rain over land for $T_B(37V)$

CHRDL = Criterion for heavy rain over land for $T_B(37V) - T_B(37H)$

CMRL = Criterion for maybe rain over land for $T_B(37V)$

CMRDL = Criterion for maybe rain over land for $T_B(37V) - T_B(37H)$

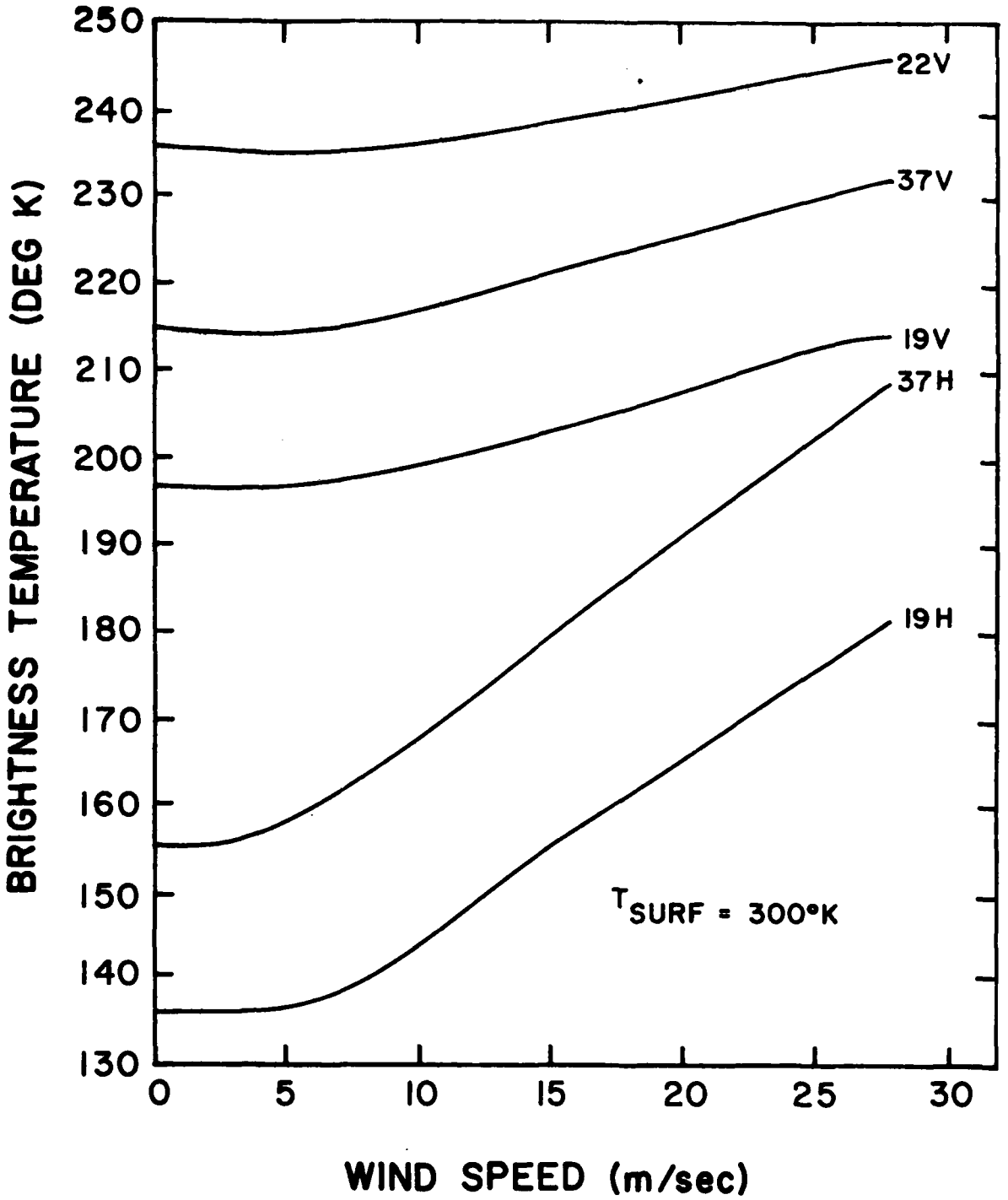

Figure IV.1 Brightness temperature as function of frequency and wind speed.

speed than the vertical channels. The SSM/I wind speed retrieval algorithm is given by

$$SW = C_{sw,o} + C_{sw,1}\, T_B(19H) + C_{sw,2}\, T_B(22V) \cdot \qquad \text{(IV.1)}$$

$$+ C_{sw,3}\, T_B(37V) + C_{sw,4}\, T_B(37H),$$

where SW is surface wind speed. The coefficients for all eleven climates are listed below:

Climate Code	$C_{sw,o}$	$C_{sw,1}$	$C_{sw,2}$	$C_{sw,3}$	$C_{sw,4}$
1	191.5600	.4903	-.4432	-.9199	.3577
2	168.3900	.5366	-.4548	-.7656	.2635
3	177.3150	.3913	-.2818	-1.0083	.4095
4	147.7600	.5077	-.3547	-.7409	.2333
5	127.1300	.4788	-.2546	-.7162	.2030
6	163.0700	.2923	-.1204	-1.0967	.4612
7	95.9940	.6106	-.3034	-.4638	.0192
8	130.4200	.3676	-.1508	-.8400	.3056
9	117.5900	.4225	-.1899	-.7096	.2081
10	130.4200	.3676	-.1580	-.8400	.3056
11	117.5900	.4225	-.1899	-.7096	.2081

IV.B.2 Precipitation Over Ocean (RO)

At lower frequencies, such as 19.35 GHz, rain is highly absorptive and results in an apparent warm brightness temperature over a cold background such as the ocean. With increasing rain rate, the difference in brightness temperature between the two polarizations at a given frequency tend to decrease. These two characteristics are demonstrated in Figure IV.2.

The SSM/I data channels selected for retrieval of rain over ocean are 19.35H, 22.235V, 37.0 V & H. The algorithm for the retrieval is given by

$$RO = C_{ro,o} + C_{ro,1}\, T_B(19H) + C_{ro,2}\, T_B(22V) \qquad \text{(IV.2)}$$

$$+ C_{ro,3}\, T_B(37V) + C_{ro,4}\, T_B(37H).$$

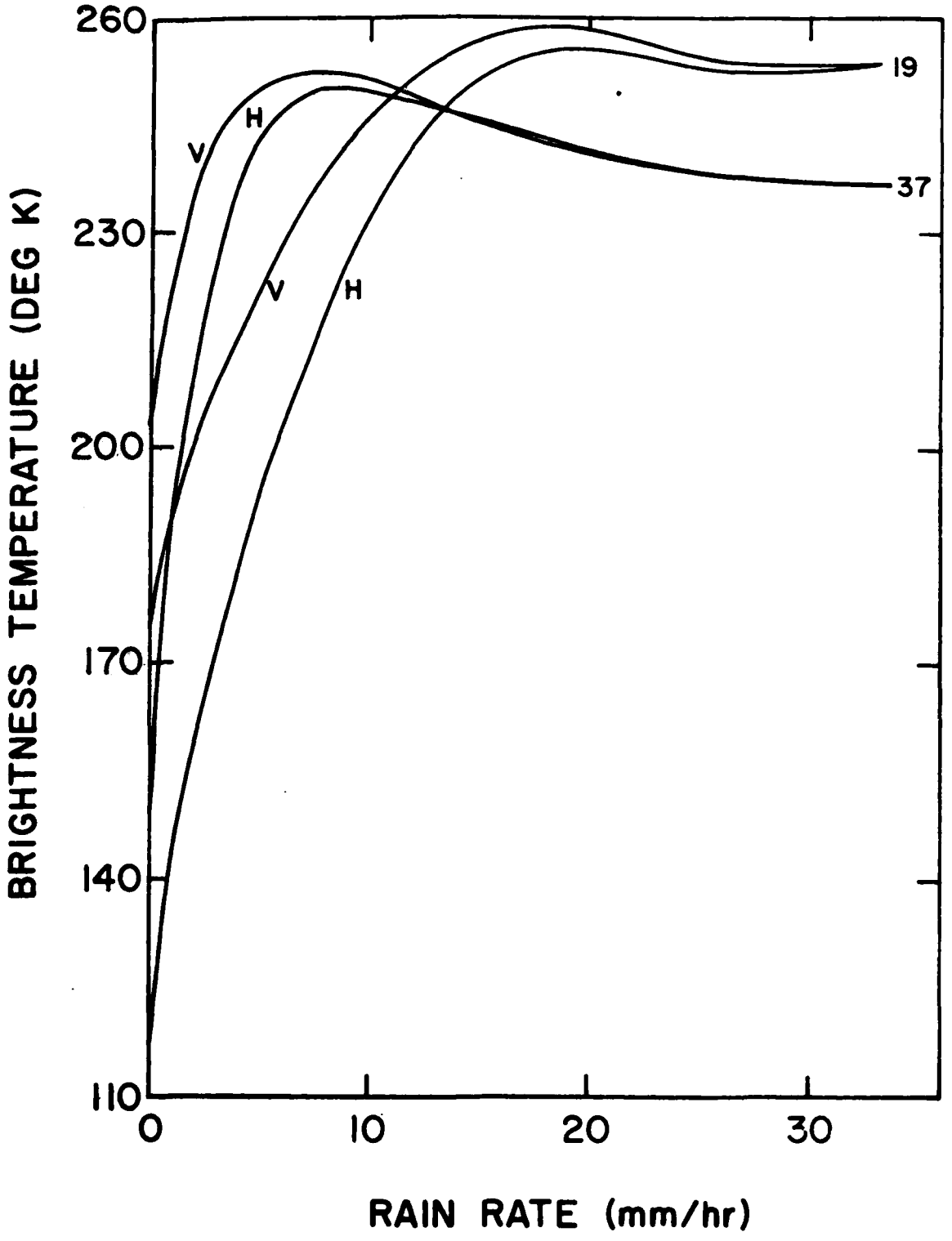

Figure IV.2 Brightness temperature vs. rain rate over mid-latitude ocean at 19 and 37 GHz

The coefficents for all climates are:

Climate code	$C_{ro,o}$	$C_{ro,1}$	$C_{ro,2}$	$C_{ro,3}$	$C_{ro,4}$
1	210.2800	.1217	-.7829	-.1830	.0998
2	215.1800	.1026	-.8059	-.1944	.1354
3	173.0400	.1938	-.6500	-.2291	.0808
4	169.2900	.1523	-.6065	-.3531	.2162
5	123.4000	.2019	-.4070	-.5117	.2969
6	135.8000	.2659	-.5170	-.2751	.0618
7	114.5500	.2708	-.6228	-.2836	.2521
8	9.5432	.1796	-.2109	.1214	-.0753
9	24.1020	.0825	.1367	-.3411	.0843
10	9.5432	.1796	-.2109	.1214	-.0753
11	24.1020	.0825	.1367	-.3411	.0843.

IV.B.3 Cloud Water (CWO) and Liquid Water (LWO) Over Ocean

The SSM/I retrieval algorithm for liquid water in the atmosphere includes two separate components. One of these, CWO, retrieves the amount of liquid water contained in cloud droplets, defined to be less than 100 m in diameter. The dominant radiative process for droplets of this size range is absorption for the SSM/I frequencies. The response at 19.35, 22.235 and 37 GHz to integrated cloud water over a mid-latitude ocean background is shown in Figure IV.3. The data channels selected for the retrieval of CWO are the same as for all the other ocean parameters, i.e., 19.35 H, 22.235 V, 37H and V.

$$CWO = C_{cwo,o} + C_{cwo,1}\, T_B(19H) + C_{cwo,2}\, T_B(22V) \qquad (IV.3)$$

$$+ C_{cwo,3}\, T_B(37V) + C_{cwo,4}\, T_B(37H).$$

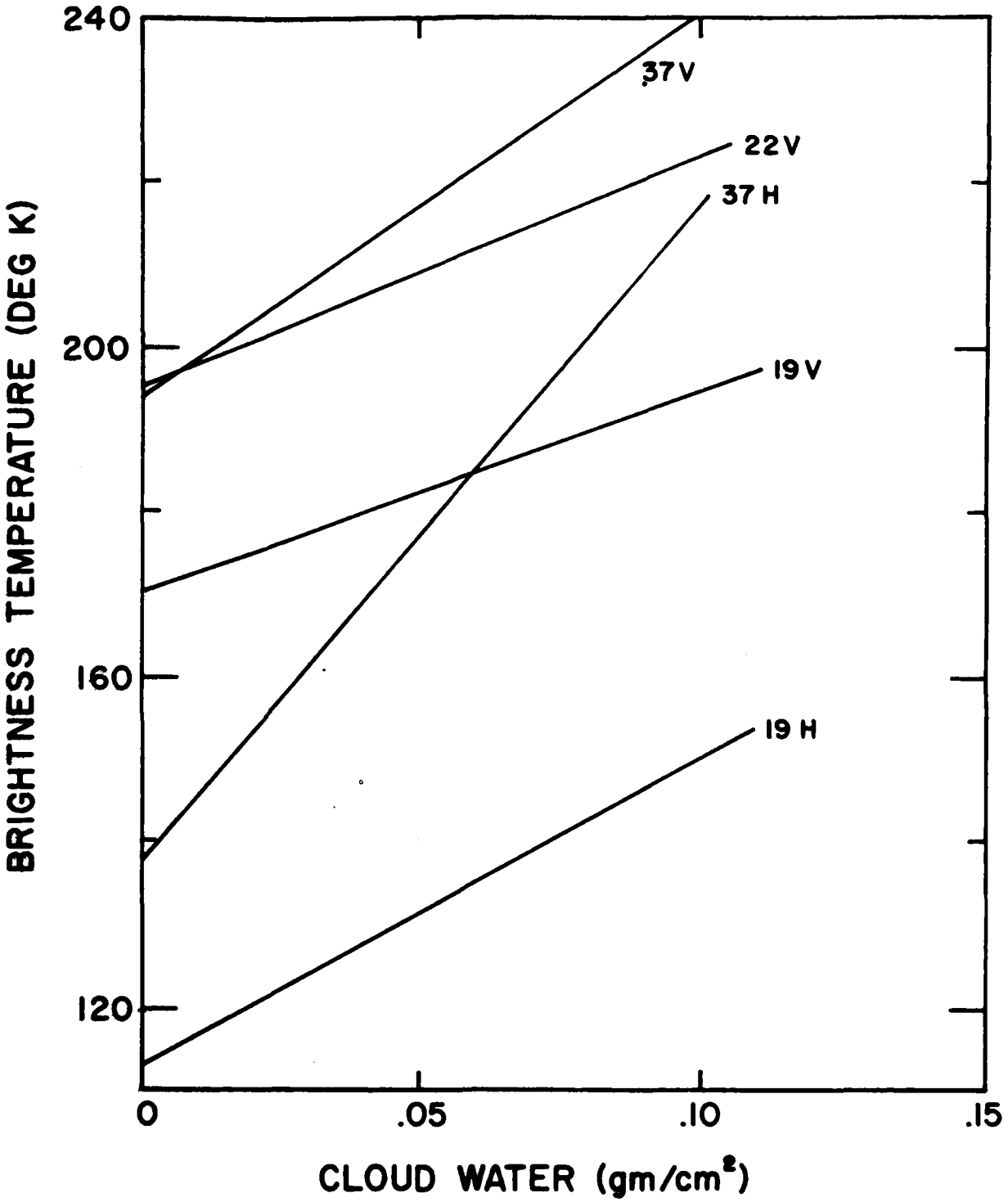

Figure IV.3 Brightness temperature vs. cloud water over mid-latitude ocean at 19, 22 and 37 GHz

The coefficients for all the climate codes are listed below:

Climate Code	$C_{cwo,o}$	$C_{cwo,1}$	$C_{cwo,2}$	$C_{cwo,3}$	$C_{cwo,4}$
1	-6.5240	-.0159	-.0044	.0407	.0045
2	-6.5292	-.0151	-.0046	.0408	.0041
3	-6.2070	-.0141	-.0038	.0383	.0035
4	-6.1372	-.0094	-.0054	.0398	-.0003
5	-5.7451	-.0037	-.0062	.0387	-.0047
6	-5.8903	-.0123	-.0031	.0358	.0025
7	-6.1411	-.0007	-.0061	.0395	-.0059
8	-4.0977	-.0066	-.0013	.0230	.0020
9	-3.6289	-.0047	-.0021	.0212	.0011
10	-4.0977	-.0066	-.0013	.0230	.0020
11	-3.6289	-.0047	-.0021	.0212	.0011

The other liquid water retrieval algorithm for the ocean is designed to retrieve the integrated liquid water contained in drops of diameter greater than 100 m, i.e., the dimensions of rain drops. The regression equation for the retrieval of LWO is

$$LWO = C_{lwo,o} + C_{lwo,1}\, T_B(19H) + C_{lwo,2}\, T_B(22V) + C_{lwo,3}\, T_B(37V) + C_{lwo,4}\, T_B(37H), \quad \text{(IV.4)}$$

where the coefficient for the eleven climates are as follows:

Climate Code	$C_{lwo,o}$	$C_{lwo,1}$	$C_{lwo,2}$	$C_{lwo,3}$	$C_{lwo,4}$
1	50.7180	.0300	-.1881	-.0493	.0285
2	53.9140	.0259	-.2053	-.4830	.0374
3	40.7175	.0405	-.1353	-.0768	.0289
4	39.4580	.0344	-.1226	-.0844	.0342
5	25.0010	.0429	-.0399	-.1205	.0310
6	30.7170	.0510	-.0824	-.1043	.0293
7	34.6250	.0474	-.0592	-.1749	.0623
8	.3091	.0209	-.0049	-.0037*	-.0142
9	-.8477	.0048	.0177	-.0137	-.0014
10	.3091	.0209	-.0049	.0037*	-.0142
11	-.8477	.0048	.0177	-.0137	-.0014

*The difference in sign of the two numbers with asterisks is apparently a mistake. The Fleet Numerical Oceanography Center and subsequently Hughes Aircraft Company have been notified of this error.

IV.C Land Retrievals

IV.C.1 Soil Moisture (SM)

The emissivity of soil for various surface soil moisture contents is shown in Figure IV.4 for the 1.43, 19 and 37 GHz frequencies. The 19.35 V & H GHz channels are selected for the retrieval of soil moisture. The retrieval algorithm for soil moisture is given by

$$SM = C_{sm,0} + C_{sm,1}\, T_B(19V) + C_{sm,2}\, T_B(19H). \qquad (IV.5)$$

The coefficients for all the climate codes are defined as follows:

Climate Code	$C_{sm,o}$	$C_{sm,1}$	$C_{sm,2}$
1	121.3000	-0.4596	0.0839
2	108.8100	-0.3877	0.0494
3	109.5830	-0.3872	0.0414
4	89.9820	-0.2924	0.0058
5	71.1540	-0.1970	-0.0378
6	97.8660	-0.3148	-0.0011
7	85.8390	-0.2818	-0.0040
8	67.3730	-0.1483	-0.0874
9	0	0	0
10	63.5920	-0.0995	-0.1370
11	0	0	0

For the polar cold season and the upper-latitude cold season transition zones (Climate Code 11 and 9), land is regarded as frozen and soil moisture is not retrieved.

IV.C.2 Precipitation Over Land (RL)

The calculated brightness temperature at 37 and 85.5 GHz due to rain over land at mid-latitudes is given in figure IV.5. Rain causes a reduction in the apparent brightness temperature over the warm land background because the back scatter of the cold upper atmosphere begins to dominate the forward scatter from the land surface and the self emission from the atmosphere. This effect is absent over the ocean due to the much lower ocean background

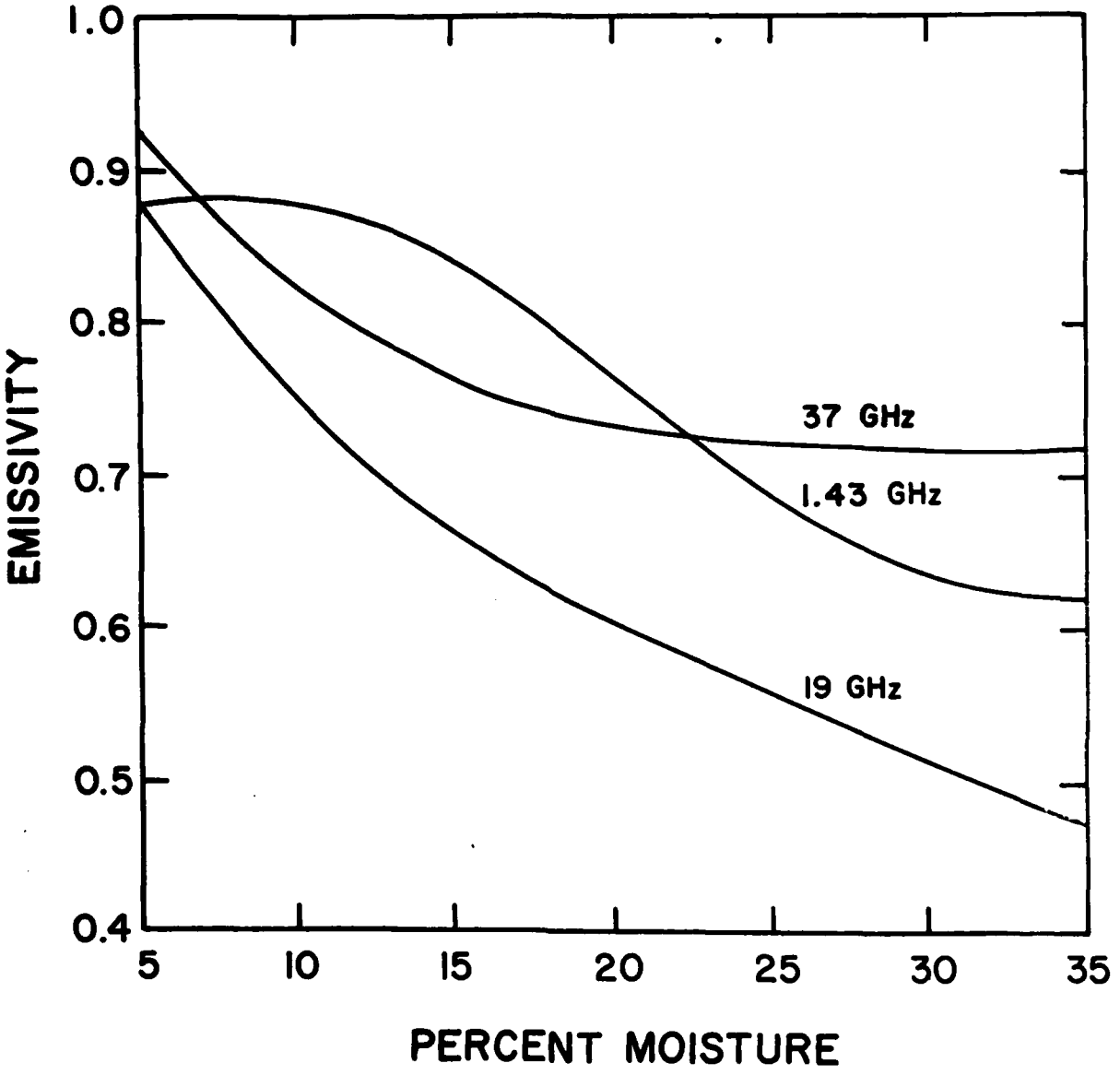

Figure IV.4 Emissivity at 1.43, 18 and 37 GHz vs. soil moisture

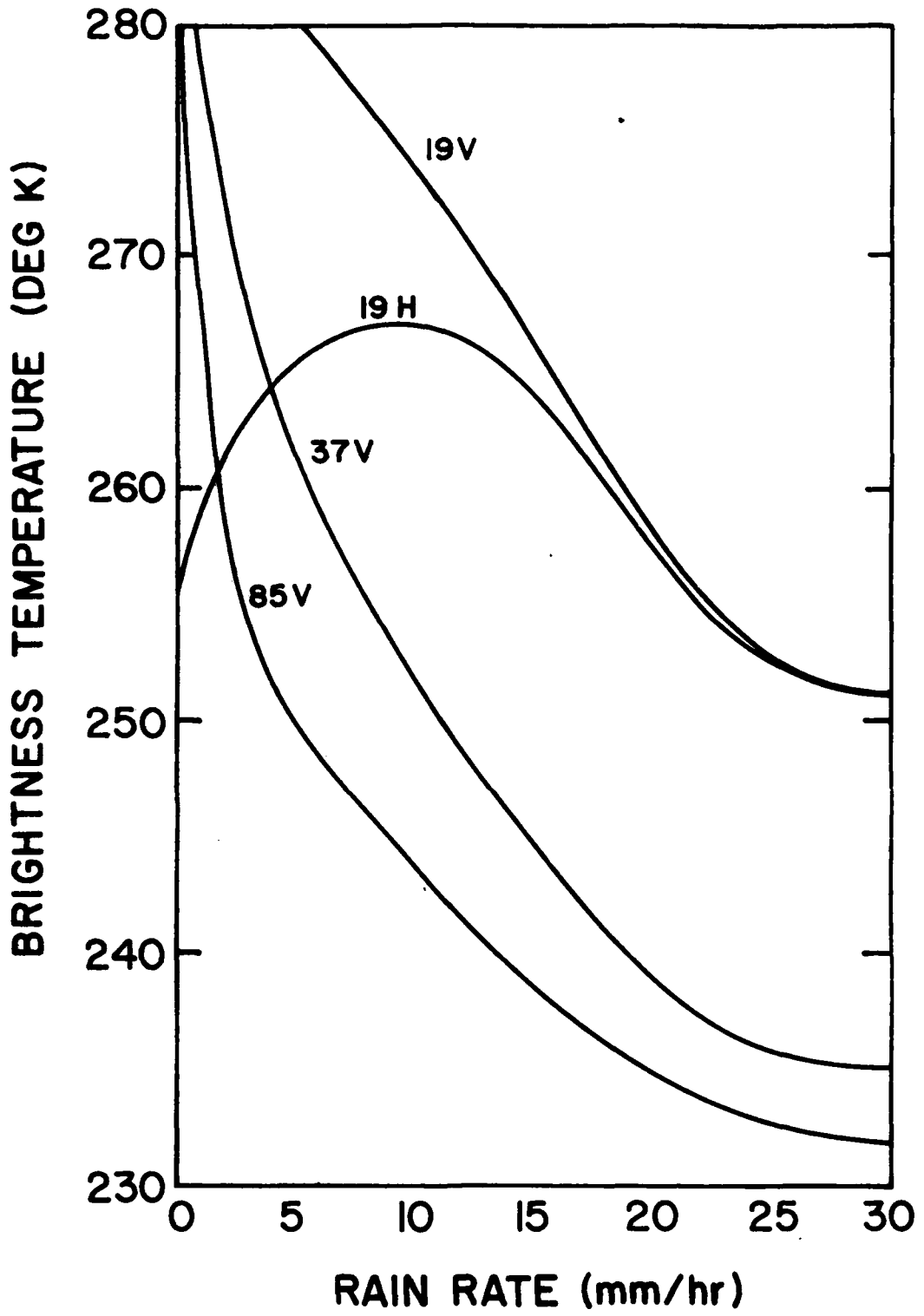

Figure IV.5 Brightness temperature vs. rain rate over mid-latitude land at 19, 37 and 85 GHz

and the coefficients are listed below:

Climate Code	$C_{lwl,0}$	$C_{lwl,1}$	$C_{lwl,2}$
1	53.1520	-0.1495	-0.0471
2	57.2120	-0.1405	-0.0713
3	51.3090	-0.1580	-0.0315
4	49.7870	-0.0977	-0.0873
5	42.3610	-0.0548	-0.1032
6	49.4650	-0.1665	-0.0158
7	52.2480	-0.0687	-0.1278
8	29.7660	-0.0381	-0.0725
9	0	0	0
10	17.1110	-0.0213	-0.0417
11	0	0	0

Since liquid water does not generally exist in polar and sub-polar regions during the cold season, liquid water over land is not retrieved for climate codes 11 and 9.

IV.C.4 Cloud Water Over Land (CWL)

Cloud water over land is much more difficult to retrieve than cloud water over the ocean (6,7) because the land background is much warmer than the ocean. As a result, at the lower frequencies there is little sensitivity to cloud water. Besides, the land background is more variable (7) than the ocean. The brightness variation due to cloud water is of the same order of magnitude as the noise level of the land surfaces. On the other hand, the higher frequency channels tend to be so sensitive to cloud water that they serve better as indicators of the existence of clouds than of cloud water content (6). The algorithm developed for the SSM/I retrieval of CWL is given by

$$CWL = C_{cwl,o} + C_{cwl,1}\, T_B(19V) + C_{cwl,2}\, T_B(19H) + C_{cwl,3}\, T_B(37V) + C_{cwl,4}\, T_B(85V). \quad \text{(IV.8)}$$

The coefficients used in retrieval for all the climates are defined below:

Climate Code	$C_{cwl,o}$	$C_{cwl,1}$	$C_{cwl,2}$	$C_{cwl,3}$	$C_{cwl,4}$
1	.6221	.0036	-.0031	.0251	-.0268
2	1.6545	-.0008	-.0006	.0362	-.0384
3	.8821	.0006	-.0007	.0271	-.0283
4	1.5350	.0014	-.0030	.0362	-.0377
5	1.4154	.0036	-.0054	.0362	-.0369
6	1.1421	-.0024	.0017	.0290	-.0298
7	1.2078	-.0050	.0033	.0415	-.0401
8	1.5366	.0002	-.0019	.0328	-.0342
9	.9329	-.0045	.0028	.0351	-.0333
10	1.6578	-.0033	.0017	.0294	-.0314
11	.6579	-.0040	.0023	.0286	-.0265

IV.D Ice Retrievals

The SSM/I retrieval algorithm for ice is derived differently than those for ocean and land retrievals. Certain relationship among the brightness temperatures and ice parameters were predetermined (See Equations III.48-50), and coefficients of these relationship are derived through analytic expressions and climatological data as described in subsection III.C.3. The coefficients A_o and A_1 from equation III.4.8 and C_o, C_1, C_2 from equation III.50 for the derivation of ice concentration, IC, and the effective average ice brightness temperature, T_x, are listed below:

	A_o	A_1	C_o	C_1	C_2	T_c(MY)
Polar-cool	1.1880	-0.0176	-219.0600	1.1050	193.6400	228.00
Polar-cold	1.1780	-0.0176	-217.7000	1.1050	192.2800	218.00

where T_c(MY) is the critical temperature for the determination of ice type. If T_x is greater than T_c(MY), the ice is defined to be first year, otherwise it is designated to be MY ice.

Cloud water over ice (CWI) is retrieved by the SSM/I algorithm even though it is not required by the specifications. The data channels employed are 19.35 V & H and 37.0 V & H.

$$CWI = C_{cwi,o} + C_{cwi,1}\, T_B(19V) + C_{cwi,2}\, T_B(19H) \qquad \text{(IV.9)}$$

$$+ C_{cwi,3}\, T_B(37V) + C_{cwi,4}\, T_B(37H).$$

The coefficients employed are listed below.

	$C_{cwi,o}$	$C_{cwi,1}$	$C_{cwi,2}$	$C_{cwi,3}$	$C_{cwi,4}$
Polar-cool	.3415	-.0010	-.0048	-.0667	.0744
Polar-cold	-.2082	-.0003	-.0121	-.0320	.0468.

REFERENCES

1. Hollinger, J. P., and R. C. Lo, "SSM/I Project Summary Report", Naval Research Laboratory, Technical Memorandum Report 5055; April 1983.

2. "Special Sensor Microwave/Imager (SSM/I) Critical Design Review, Vol. II. Ground Segment", Contract No. F04701-79-C-0061, Hughes Aircraft Company, March 1980.

3. "Special Sensor Microwave/Imager (SSM/I) Computer Program Development Specification (Rev.B) (Specification for FNWC)", Contract No. F04701-79-C-0061, CDRL Item No. 016A2, Hughes Aircraft Company, July 1980.

4. "Special Sensor Microwave/Imager (SSM/I) Computer Program Product Specification (Specification for FNOC), Volume III Environmental Parameter Extraction, Computer Program Component (SMIEPE)", Contract No. F04701-79-C-0061, CDRL Item No. 018A2, Hughes Aircraft Company, December 1980.

5. "Special Sensor Microwave/Imager (SSM/I) Data Requirement Document DRD for AFGWC", Contract No. F04701-79-C-0061, CDRL Item No. 028A2, Hughes Aircraft Company, January 1981.

6. "Proposal for Microwave Environmental Sensor System (SSM/I), Vol. I Technical Proposal", RFP No. F0471-78-R-0094, Hughes Aircraft Company, January 1979.

7. Burke, H, K., and K. C. Jones, "Models of Environmental Parameters for the SSM/I Program", Environmental Research and Technology, Inc., February 1980.

8. Burke, H. K., et.al., "Inversion Algorithms for Environmental Parameter Extraction of the SSM/I Program", Environmental Research and Technology, Inc., February 1980.

9. Gaut, N. T., and Reifenstein III, "Interaction Model of Microwave Energy and Atmospheric Variables", Final Report, Environmental Research and Technology, Inc., Concord, Massachusetts, 1971.

10. Sze, N. D., "Variational Methods in Radiative Transfer Problems", J. Current Spectro. Radiat. Transfer, Vol. 16, 1976.

11. Burke, H. K., and N. D. Sze, "A Comparison of Variational and Discrete Ordinate Methods for Solving Radiative Transfer Problems", J. Current Spectro. Radiat. Transfer, Vol. 17, 1977.

12. Gaut, N. E., "Studies of Atmospheric Water Vapor by Means of Passive Microwave Techniques", Research Laboratory for Electronics, Tech. Report 467, Massachussetts Institute of Technology, 1968.

13. Van Vleck, J. H., and V. F. Weisskopf, "On the Shape of Collision Broadened Lines", Rev. Mod. Phys., Vol. 17, 1945.

14. Staelin, D. H., et.al., "Remote Sensing of Atmospheric Water Vapor and Liquid Water with the NIMBUS-5 Microwave Spectrometer", J. Appl. Met, Vol. 15, pp. 1203-1214, 1976.

15. Rosenkranz, P. W., "Shape of the 5 mm Oxygen Band in the Atmosphere", IEEE Trans. Antenna and Propagation, Vol. AP-23, No. 4, 1975.

16. Lewis, J. O., and D. A. Parson, "The Relation of Raindrop Size to Intensity", Trans. American Geophys. Union, Vol. 24, p. 452, 1943.

17. Burke, H. K., and K. C. Jones, "Models of Environmental Parameters for the SSM/I Program", Environmental Research and Technology, Inc., February 1980.

18. Lane, J. A., and J. A. Saxton, "Dielectric Dispersion in Pure Polar Liquids at Very High Radio Frequencies", Proc. Roy. Soc., London A, 214, pp. 531-545, 1952.

19. Chang, A. T. C., and T. Wilheit, "Remote Sensing of Atmospheric Water Vapor, Liquid Water, and Wind Speed at the Ocean Surface by Passive Microwave Techniques from the NIMBUS-5 Satellite", Radio Science, 1979.

20. Cardone, V. J., "Specification of the Wind Field Distribution in the Marine Boundary Layer for Wave Forecasting", Report TR 69-1, Geophysical. Sci. Lab., New York University, 1969.

21. Wilheit, T. T., "A Model for the Microwave Emissivity of the Ocean's Surface as a Function of Wind Speed", NASA TM 80278, 1979.

22. Cox, C. and W. Munk, "Measurement of the Roughness of the Sea Surface from Photographs of the Sun's Glitter", J. Optical Society of America, Vol. 44, No. 11, 1955.

23. Stogryn, A., "The Brightness Temperature of a Vertically Structured Medium", Radio Science, Vol. 5, No. 12, pp. 1397-1406, 1970.

24. Burke, W. J., and J. F. Paris, "A Radiative Transfer Model for Microwave Emission from Bare Agricultural Soils", NASA Tech. Memo. X-58166, NASA Johnson Space Center, Houston, Tex., 1975.

25. Wang, J., et.at., "Dielectric Constants of Soil Microwave Frequencies, II", NASA Tech. Pap. TP-1238, 1978.

26. Geiger, F., and D. Williams, "Dielectric Constants of Soils at Microwave Frequencies", Contract NASA X-652-72-238, NASA Goddard Space Flight Center, Greenbelt, Maryland, 1972.

27. Choudhury, B. J., T. J. Schmugge, A. Cheng, and R. W. Newton, "Effect of Surface Roughness on the Microwave Emission from Soil", J. of Geophy. Res., Vol. 84, No. C9, 1979.

28. Gloerson, P., et.al., "Time-Dependence of Sea-Ice Concentration and Multiyear Ice Fraction in the Arctic Basis", J. Boundary-Layer Met., Vol. 13, 1978.

29. "Special Sensor Microwave/Imager (SSM/I) Data Requirement Document DRD for AFGWC", Hughes Aircraft Company, Contract No. F04701-79-C-0061, CDRL Item No. 028A2, January 1981.

END

FILMED

11-83

DTIC